
Group-Aware Matrix Estimation and Latent Subspace Recovery

Hamza Golubovic*

Department of Statistics,
Columbia University
New York, NY 10027
hg2723@columbia.edu

Matthew Shen*

Department of Statistics,
Columbia University
New York, NY 10027
ms7079@columbia.edu

Genevera I. Allen

Department of Statistics,
Irving Institute for Cellular Dynamics,
Zuckerman Institute
Columbia University
New York, NY 10027
genevera.allen@columbia.edu

Tarek M. Zikry†

School of Data and Information Sciences,
University of North Carolina at Chapel Hill
Chapel Hill, NC 27599
tarek@unc.edu

Abstract

Modern matrix completion problems often involve heterogeneous data whose rows simultaneously belong to many meta-categories, such as demographic and age groups in recommendation systems, or region and recording session labels in neural electrophysiological experiments. Standard low-rank estimators impose a single global latent geometry, which can recover average structure but may smooth away subgroup-specific variation, especially when observations are unevenly distributed across groups. We introduce Group-Aware Matrix Estimation (GAME), a convex estimator for overlapping subgroup-wise low-rank matrix estimation. GAME regularizes category-specific submatrices through overlapping nuclear-norm penalties, allowing related groups to borrow information while preserving local latent structure in a shared coordinate system. We provide finite-sample guarantees for both reconstruction error and subgroup-specific subspace recovery, showing how performance depends on sampling density, subgroup rank, and overlap structure. Experiments on synthetic, recommendation, ecological, and neuroscience datasets show that GAME is most beneficial in structured missingness regimes, where subgroup-aware regularization improves both reconstruction accuracy and latent subspace fidelity. Across these benchmarks, GAME is competitive or best among global low-rank, side-information, and modern imputation baselines, with the largest gains when subgroups exhibit distinct low-rank structure.

1 Introduction

In recommendation systems, users may belong to overlapping demographic groups such as age, gender, and occupation [Harper and Konstan, 2015]. In biological, experimental, and longitudinal studies, samples may be indexed by subject, batch, session, spatial region, or other partially overlapping sources of variation [Wang and Lock, 2024, Chen et al., 2024]. In such settings, the goal is often not only to reconstruct missing entries accurately on average, but also to preserve

*These authors contributed equally.

†Corresponding author.

subgroup-specific latent structure that may be scientifically or operationally important. Standard nuclear-norm estimators impose a single global low-rank penalty [Candes and Recht, 2008], which can smooth away subgroup-specific variation - especially for groups that are unevenly or weakly observed, where faithful estimation often matters most. More broadly, heterogeneous data need not conform to one shared low-rank geometry; different subgroups may exhibit local low-dimensional structure that is related through overlap but not identical [Candes and Recht, 2008]. This motivates an overlap-aware estimator that shares information across groups while preserving local structure.

In this work, we propose Group-Aware Matrix Estimation (GAME), a convex framework for heterogeneous matrix estimation with overlapping meta-categories. GAME (Figure 1) balances faithful reconstruction of the observed entries with nuclear-norm regularization on meta-category-defined submatrices, allowing local low-rank structure to be learned within groups while overlap propagates information across them. This yields a single coherent estimate that borrows strength across groups without forcing all groups into the same latent subspace.

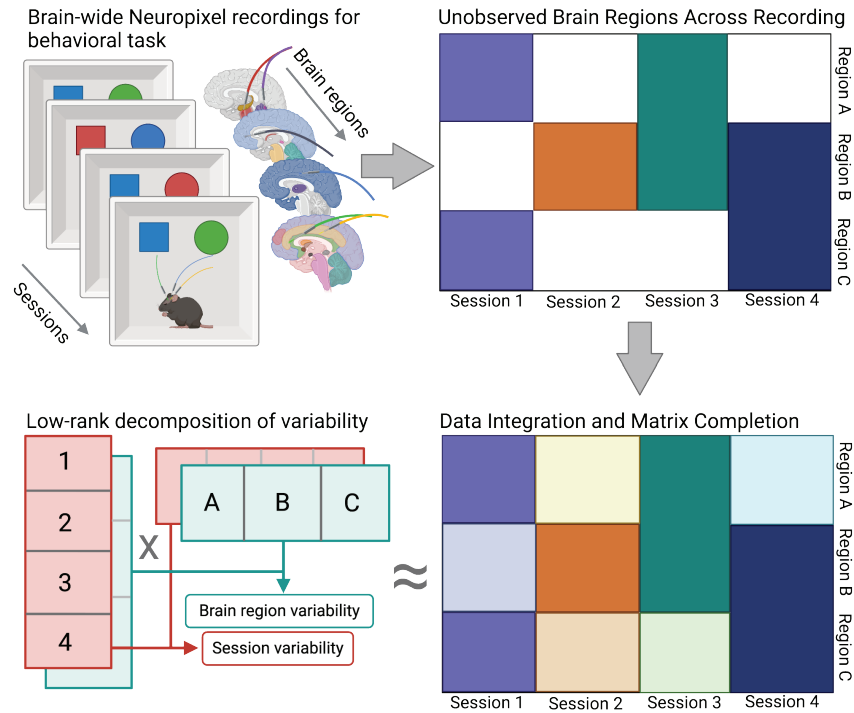


Figure 1: **Overview of motivating group-aware matrix estimation in neuroscience.** Brain-wide Neuropixel recordings measure single-neuron temporal responses to stimuli in mice and monkeys, but can only measure a small number of brain regions at once, leaving large block-missingness across recording sessions and brain regions. We develop Group Aware Matrix Estimation (GAME) to impute missing region dynamics and decompose variability across meta-categories such as region and session.

GAME is a general estimator for overlapping subgroup-wise low-rank structure; it is not restricted to settings with an explicit block-sampling model. However, its inductive bias is most beneficial when subgroups exhibit distinct low-rank structure. Structured missingness is one important instance: when some subgroups are weakly observed, overlap allows underrepresented groups to borrow information without being smoothed into a single global estimate.

To optimize the GAME objective at scale, we use the proximal average framework [Bauschke et al., 2008, Yu, 2013], which avoids the auxiliary-variable and consensus overhead of ADMM in high-category settings [Boyd et al., 2011]. Beyond scalable optimization, GAME also supports analysis of subgroup-specific latent geometry: by regularizing each subgroup through an overlapping nuclear norm, the estimator supports both reconstruction and local subspace recovery.

We evaluate GAME on synthetic data with hierarchical group structure, MovieLens-100k [Harper and Konstan, 2015] under global and block-wise missingness and meta-category misspecification, multi-label birdsong classification from the BirdSet benchmark [Clapp et al., 2023, Rauch et al., 2025], and a scientific case study on multi-session Neuropixel recordings [Chen et al., 2024]. Across these settings, GAME performs competitively or best across all settings, with the largest margins when subgroups exhibit distinct low-rank structure or when the goal is to recover local latent geometry.

Contributions Together, these ideas lead to four main contributions:

- **A subgroup-aware convex estimator for heterogeneous matrix estimation.** We introduce GAME, which promotes overlapping subgroup-wise low-rank structure while maintaining a shared coordinate system across the full matrix.
- **Scalable optimization without consensus overhead.** We develop a proximal-averaging solver for the GAME objective that is practical in settings with many overlapping categories.
- **Provable reconstruction and subspace fidelity under overlap.** We provide finite-sample guarantees for both reconstruction error and subgroup-specific subspace recovery, clarifying how performance depends on sampling, rank, and overlap structure.
- **Empirical validation on synthetic and real datasets.** We show that GAME performs competitively or better than benchmark methods across diverse settings, with the largest gains in structured missingness regimes. On Neuropixels data, GAME recovers region-specific latent dynamics, illustrating value beyond aggregate imputation accuracy.

The remainder of the paper develops the formulation, optimization, and theory, followed by experiments on synthetic and real data.

2 Related Work

2.1 Matrix Completion with Side Information

Low-rank matrix completion has been extensively studied as a framework for recovering low-rank matrices from partial observations. Classical formulations rely on the assumption that the target matrix is globally low-rank and can be recovered via a convex relaxation using the nuclear norm [Candes and Recht, 2008, Recht et al., 2010]. Non-convex approaches, such as alternating least squares (ALS) [Hastie et al., 2014, Mazumder et al., 2010] have also been widely adopted for their computational efficiency on high-dimensional matrices. While these models enjoy strong theoretical guarantees under incoherence and random sampling assumptions [Candes and Plan, 2010, Negahban and Wainwright, 2011], they treat all rows and columns equally, and do not incorporate meta (i.e. “side”) information that may be readily available in real-world applications.

Several methods incorporate *side information*—row or column features—into the completion problem. Note that *side information* is analogous to *meta-category*. Inductive Matrix Completion (IMC) [Jain and Dhillon, 2013] assumes that the target matrix admits a factorization of the form

$$\mathbf{X} \approx \mathbf{A}\mathbf{M}\mathbf{B}^\top,$$

where \mathbf{A} and \mathbf{B} are known feature matrices and \mathbf{M} is a low-rank parameter matrix to be learned. The feature matrices may contain one-hot encodings of categorical information or singular vectors of a cheaply completed matrix approximation of \mathbf{X} . Similar to IMC, Maxide [Xu et al., 2013] exploits side information by restricting the target matrix to lie in the subspaces spanned by known feature matrices, but penalizes the completion problem with a lower-dimensional trace-norm, yielding substantial computational and sample-complexity gains when the side information is well-aligned with the latent structure. DirtyIMC [Chiang et al., 2015] addresses noisy or incomplete side information by augmenting IMC with a low-rank residual term, while FNNM [Yang et al., 2022] instead decomposes the target into a globally low-rank component and a sparse component tied to the side information, balancing global and local structure via nuclear norm and ℓ_1 regularization jointly. [Chang et al., 2025] observe that when side information is incomplete, the component of the target matrix lying outside the available feature subspaces lacks any inherent low-rank structure and must be explicitly regularized, proposing to penalize the nuclear norm of this orthogonal complement projection alongside the global nuclear norm.

2.2 Issues with Side Information Methods

A common theme across these side-information methods is that each imposes a specific *generative* assumption about how features produce entries: a bilinear factorization through known feature matrices in IMC and Maxide, augmented by a low-rank residual in DirtyIMC, a sparse correction in FNNM, or an orthogonal-complement penalty in [Chang et al., 2024]. When this commitment is misspecified, the estimator converges not to the truth but to its projection onto the assumed model class. In other words a side-information method given misleading features is biased toward a wrong target, whereas standard matrix completion given no features simply returns the best low-rank fit. This concern is sharpened in the categorical setting: encoding group membership as one-hot row features collapses a bilinear model $\mathbf{X} \approx \mathbf{A}\mathbf{M}\mathbf{B}^\top$ to a per-group mean model, in which every row in a category is identical up to noise. The natural workaround is supplementing the one-hot encoding with leading singular vectors of a cheaply imputed approximation of \mathbf{X} . However, it quickly becomes unclear how many singular vectors to retain for each category, becoming an unprincipled hyperparameter without theoretical guarantees.

These limitations motivate our GAME approach, which makes no commitment about data generation, robust even when side-information is weak/noisy. Categorical meta-information is used not to model how entries arise from features, but only to define a partition of the rows of \mathbf{X} under which each block is hypothesized to be approximately low-rank (a purely observational condition). When this hypothesis is misaligned with the data, the truth still lies in the model class (in particular, the globally low-rank case is recoverable through the interpretable λ_c), so the estimator has at most a tuning inefficiency rather than the structural bias incurred by a misspecified bilinear model.

2.3 Low-rank estimation and latent structure in heterogeneous data

Low-rank and latent-structure methods are widely used when high-dimensional observations admit a more compact representation. In some heterogeneous settings, this structure may be better described by multiple low-dimensional components rather than a single shared subspace. For example, subspace clustering and low-rank representation methods explicitly model data as arising from a union of low-dimensional subspaces [Elhamifar and Vidal, 2013, Liu et al., 2013]. In related multi-task settings, shared low-dimensional representations can improve learning across related tasks [Argyriou et al., 2008, Obozinski et al., 2011]. More broadly, recent work in high-dimensional biology has emphasized that jointly modeling structured variation across multiple sample sets can be more powerful and scientifically informative than analyzing each dataset separately [Wang and Lock, 2024].

These perspectives are relevant when the goal is not only reconstruction, but also recovering latent structure that organizes heterogeneous observations. In such settings, the latent representation can support downstream tasks such as segmentation, integration across cohorts, or prediction from partially observed data. This setting arises when different groups are weakly observed but still share enough structure to support information transfer.

Neural population recordings provide one important instance of this broader problem (Figure 1). Recent methods use low-rank or latent-variable structure to denoise, compress, and interpret large-scale neural data. Penalized matrix decomposition can separate low-dimensional signal from noise in functional imaging data [Buchanan et al., 2018], while tensor decompositions reveal structure across temporal, spatial, and experimental axes [Pellegrino et al., 2024, Williams et al., 2018]. Latent factor models such as GPFA and LFADS instead impose explicit temporal structure on neural dynamics [Yu et al., 2009, Pandarinath et al., 2018], and post-hoc alignment methods compare low-dimensional dynamics across conditions or animals [Dabagia et al., 2022]. Recent multi-session and multi-animal models further show that shared latent structure can improve inference or prediction across partially observed recordings [Azabou et al., 2024, Zhang et al., 2024, 2025, Xia et al., 2025]. However, these approaches typically assume a single shared latent space or require aligned recordings across sessions, and do not regularize overlapping subgroup-specific low-rank structure within a unified matrix estimation framework.

3 Group-Aware Matrix Estimation (GAME)

We introduce Group-Aware Matrix Estimation (GAME), a convex estimator designed to leverage overlapping categorical structures, promoting group-wise low-rank reconstructions while preserving

We defer proofs and technical details regarding semi-orthogonality and proximal derivations of the GAME algorithm (Algorithm 1) to Appendix A. With these results, we are able to obtain convergence guarantees from [Yu, 2013], highlighted in Theorem 3.1.

We use the abbreviation $\overline{L}^2 := \sum_{c \in \mathcal{C}} \lambda_c L_c^2 = \sum_{c \in \mathcal{C}} \lambda_c r \| \mathbf{D}_c \|_{\text{op}}^2$ in the following theorem to denote the weighted sum of per-category Lipschitz constants.

Theorem 3.1 (Theorem 1 of [Yu, 2013]). *Let \mathbf{W}_0 be the initialization of the PA-APG algorithm and $\widehat{\mathbf{W}}$ denote the GAME estimator from (1). Fix the accuracy $\epsilon > 0$. Let step size $\gamma = \min\{1, 2\epsilon/\overline{L}^2\}$. After at most $k = \sqrt{\frac{2}{\gamma\epsilon}} \|\mathbf{W}_0 - \widehat{\mathbf{W}}\|_F^2$ steps, the PA-APG approximation, $\widetilde{\mathbf{W}}_k$, satisfies*

$$f(\widetilde{\mathbf{W}}_k) + \bar{g}(\widetilde{\mathbf{W}}_k) \leq f(\widehat{\mathbf{W}}) + \bar{g}(\widehat{\mathbf{W}}) + 2\epsilon.$$

3.3 Theoretical Guarantees of GAME

We now establish finite-sample guarantees for GAME (1) under a partially observed noisy matrix model. We observe a uniformly i.i.d. sample Ω of N entries from $[n] \times [m]$ of the matrix $\mathbf{X} = \mathbf{W}^* + \mathbf{E}$, and analyze the non-spiky restricted estimator

$$\widehat{\mathbf{W}} \in \arg \min_{\mathbf{W} \in \mathcal{F}(\alpha^*)} \frac{1}{2} \|\mathcal{P}_\Omega(\mathbf{X} - \mathbf{W})\|_F^2 + \sum_{c \in \mathcal{C}} \lambda_c \|\mathbf{W}_c\|_*, \quad (2)$$

where $\mathcal{F}(\alpha^*) := \{\mathbf{W} : \|\mathbf{W}\|_\infty \leq \alpha^*/\sqrt{nm}\}$.

For each meta-category $c \in \mathcal{C}$, $\mathbf{W}_c := \mathbf{W}[I_c, :] \in \mathbb{R}^{n_c \times m}$ with $n_c := |I_c|$, $d_c := n_c + m$, and $r_c := \text{rank}(\mathbf{W}_c^*)$. The per-block sample count is $N_c := |\Omega \cap (I_c \times [m])|$. Row overlap multiplicity is $\kappa(i) := |\{c : i \in I_c\}|$, with extremes κ_{\max} and κ_{\min} . We now make the following assumptions.

Assumption 3.2 (Subexponential Noise). The entries E_{ij} are independent, mean zero, and subexponential with parameters (σ, R) : $\mathbb{E}[E_{ij}^p] \leq \frac{p!}{2} R^{p-2} \sigma^2$ for every integer $p \geq 2$.

Assumption 3.3 (Non-Spikiness). There is $\alpha^* \geq 1$ such that $\sqrt{nm} \|\mathbf{W}^*\|_\infty \leq \alpha^* \|\mathbf{W}^*\|_F$, and the optimization is restricted to $\mathcal{F}(\alpha^*)$.

Assumption 3.4 (Cover). $\bigcup_{c \in \mathcal{C}} I_c = [n]$, i.e. $\kappa_{\min} \geq 1$.

The spikiness constraint rules out matrices whose mass is concentrated on a small number of entries, pathological cases not identifiable from partial observations [Negahban and Wainwright, 2011].

Theorem 3.5 (GAME Frobenius Error). *Suppose Assumptions 3.2–3.4 hold and that $N n_{\min}/n \gtrsim (n+m) \log(n+m)$ with $n_{\min} := \min_c n_c$. The choice*

$$\lambda_c \gtrsim \frac{\sigma}{\kappa_{\min}} \sqrt{\frac{(N n_c/n) \log d_c}{\min(n_c, m)}} + \frac{R \log d_c}{\kappa_{\min}} \quad \forall c \in \mathcal{C} \quad (3)$$

yields, with high probability, the restricted GAME estimator $\widehat{\mathbf{W}}$ from (2) satisfying

$$\frac{\|\widehat{\mathbf{W}} - \mathbf{W}^*\|_F^2}{nm} \lesssim \frac{\kappa_{\max}^2}{\kappa_{\min}^3} \cdot \frac{\sigma^2 \log(n+m)}{N} \sum_{c \in \mathcal{C}} r_c (n_c \vee m), \quad (4)$$

in the matrix-completion regime where $nm \log(n+m)/N \lesssim (\frac{R}{\sigma})^2$.

The proof is given in Appendix B. The bound from Theorem 3.5 bounds the Frobenius error of the GAME estimator and the ground truth matrix \mathbf{W}^* . It further translates into a per-category latent-subspace guarantee via a Yu–Wang–Samworth variant of Davis–Kahan/Wedin [Yu et al., 2015], which is more interesting in the context of preserving underlying latent subspaces:

Corollary 3.6 (Per-Category Right-Subspace Recovery). *For each $c \in \mathcal{C}$, let \mathbf{Q}_c^* , $\widehat{\mathbf{Q}}_c \in \mathbb{R}^{m \times r_c}$ denote the top r_c right singular vectors of \mathbf{W}_c^* and $\widehat{\mathbf{W}}_c$, and let $\sigma_{c,1}$, σ_{c,r_c} be the largest and r_c -th singular values of \mathbf{W}_c^* . Under the hypotheses of Theorem 3.5, with high probability, simultaneously for every $c \in \mathcal{C}$,*

$$\min_{\mathbf{R} \in \mathcal{O}(r_c)} \|\widehat{\mathbf{Q}}_c \mathbf{R} - \mathbf{Q}_c^*\|_F \lesssim \frac{(2\sigma_{c,1} + \|\widehat{\mathbf{W}} - \mathbf{W}^*\|_F) \|\widehat{\mathbf{W}} - \mathbf{W}^*\|_F}{\sigma_{c,r_c}^2}.$$

Discussion. Theorem 3.5 and Corollary 3.6 are both prescriptive, in that they convert each λ_c and per-category sample budget N_c from free tuning parameters into quantities that can be calibrated from observable category-level statistics, and comparative, in that they identify the regime where GAME strictly improves on global nuclear-norm regularization. We analyze each in the following.

(i) *Category-specific regularization.* The choice (3) scales with three intuitive quantities: the noise level σ , the effective sample budget Nn_c/n (the expected number of observations falling in I_c), and the local block dimension d_c . In the dominant matrix-completion regime, the sub-Gaussian piece dominates and $\lambda_c \asymp \sigma \sqrt{(Nn_c/n) \log d_c / \min(n_c, m)}$. Intuitively, smaller or more sparsely covered categories should receive proportionally stronger regularization, while larger and better-sampled categories support weaker shrinkage. This is concrete guidance that replaces grid search with a noise-calibrated rule scaling with category-level summaries that are themselves measurable from data.

(ii) *Category-specific sample requirements.* The sample condition $Nn_{\min}/n \gtrsim (n+m) \log(n+m)$ exposes a per-category identifiability threshold: each category receives an effective budget $N_c \approx Nn_c/n$, and the theorem is informative only when this budget is large relative to d_c for every relevant category, in particular for the smallest. So GAME can exploit category structure only when each meta-category is sufficiently sampled. If some categories are very small, practitioners should either oversample those categories or coarsen the partition until the threshold is met.

(iii) *When GAME beats global nuclear-norm regularization.* The dominant complexity factor in (4) is $\sum_c r_c(n_c \vee m)$, which is a sum of *local* complexities, whereas the analogous bound for the standard nuclear-norm estimator (NW) [Negahban and Wainwright, 2011, Cor. 1] carries the *global* complexity $r^*(n \vee m)$ with $r^* := \text{rank}(\mathbf{W}^*)$. Holding overlap bounded ($\kappa_{\max}, \kappa_{\min} = O(1)$, i.e. every row belongs to a constant number of categories), the error ratio is

$$\frac{\text{GAME bound}}{\text{NW bound}} \asymp \frac{\sum_c r_c(n_c \vee m)}{r^*(n \vee m)}. \quad (5)$$

GAME wins whenever \mathbf{W}^* is only moderately low rank globally but substantially lower rank within meaningful categories. As a concrete example, consider rows partitioned into $|\mathcal{C}|$ equal blocks with common local rank r_{loc} and largely distinct block subspaces (so $r^* \asymp |\mathcal{C}|r_{\text{loc}}$). In the tall matrix regime $n_c \gg m$, (5) reduces to roughly $1/|\mathcal{C}|$, so GAME improves over NW by a factor of $|\mathcal{C}|$. By Corollary 3.6, the same factor carries over to per-category subspace recovery, since the conditioning constants $\sigma_{c,1}, \sigma_{c,r_c}$ depend only on \mathbf{W}_c^* and cancel in any ratio of subspace errors.

Further detailed discussion is deferred to Appendix B. Future work may develop sharper theory under separation assumptions on the category-wise right singular subspaces, characterizing regimes in which GAME offers more robust completion while better preserving category-specific latent structure.

4 Experiments

The experiments investigate the impact of subgroup-aware regularization on three fronts: (1) preserving local latent structure that global methods smooth away, (2) reconstruction accuracy under both uniform and structured missingness, and (3) downstream task performance in clustering, classification, and latent dynamics recovery. We study these questions across four experiments: synthetic clustering (Section 4.1), movie recommendation under global, block-wise, and corrupted missingness (Section 4.2), species classification from imputed acoustic features (Section 4.3), and latent neural dynamics recovery from multi-session Neuropixels recordings (Section 4.4).

Across all experiments, we compare GAME to singular value thresholding [SVT; Cai et al., 2010], alternating least squares [ALS; Jain et al., 2012], dirty inductive matrix completion [DirtyIMC; Chiang et al., 2015], Maxide [Xu et al., 2013], FNNM [Yang et al., 2022], and OCMC [Chang et al., 2025]. We restrict DirtyIMC and Maxide to using only row-wise side information, stored in matrix $\mathbf{A} \in \mathbb{R}^{n \times d_r}$, constructed to address subspace recovery. Section 4.3 additionally baselines against two modern matrix imputation methods: MissForest [Stekhoven and Bühlmann, 2011] and TabImpute [Feitelberg et al., 2026].

Hyperparameters for baseline methods are tuned via cross-validation; for the GAME weights α_c , the heuristic in Theorem 3.5 is used as initialization, with additional scaling selected by cross-validation.

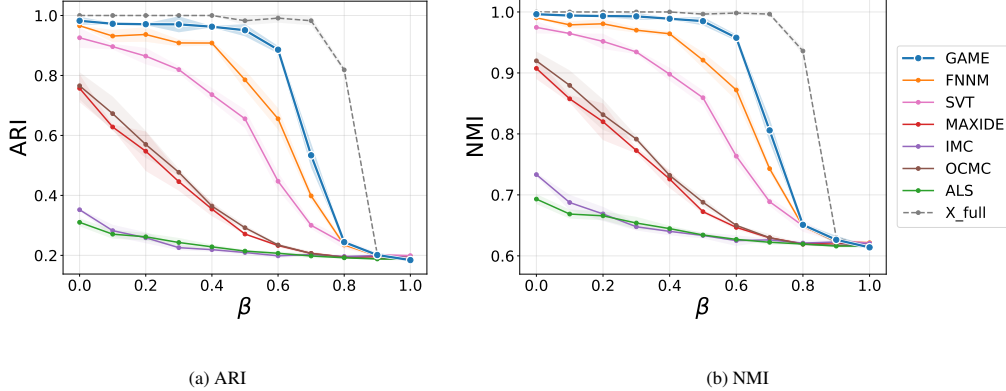


Figure 2: Synthetic clustering recovery of hidden subclusters under varying subcluster signal strength β , evaluated by ARI (\uparrow) and NMI (\uparrow). GAME nearly matches the fully observed oracle at small and moderate β , outperforming all baselines. Shaded regions denote ± 1 standard error across replications.

Additionally, when executing the iterative proximal updates for GAME, we utilized a truncated SVD to improve runtime and memory complexity, which continued to demonstrate robust performance. For most experiments, completing the matrices with GAME is computationally feasible to run locally, although for the Svoboda Lab Neuropixel dataset we resorted to implementing a GPU compatible version of GAME for large SVD computations.

4.1 Synthetic Clustering Under Subgroup Overlap

Setup. We construct a synthetic matrix $\mathbf{X} \in \mathbb{R}^{n \times m}$ with crossed group structure. Each row x_i belongs to an observed group $g \in \mathcal{G}$ and an unobserved subcluster $s \in \mathcal{S}$. The observed groups define the meta-categories available to GAME and the side-information baselines, while the hidden subclusters define the latent structure we aim to recover after matrix completion.

We set $|\mathcal{G}| = 10$, $|\mathcal{S}| = 5$, $n = 1000$, and $m = 500$. Each row is generated as

$$x_i = \mu_g + \nu_s + u_i V_g^\top + (1 - \beta) z_i W_s^\top,$$

where μ_g is a group-specific mean vector, ν_s is a subcluster-specific mean vector, V_g is a low-rank basis associated with the observed group g , and W_s is a low-rank basis associated with the hidden subcluster s . The vectors u_i and z_i are normalized Gaussian latent scores that control row-level variation within the group and subcluster components, respectively.

The parameter $\beta \in [0, 1]$ controls the strength of the hidden subcluster signal. When $\beta = 0$, the subcluster-specific low-rank component is strongest; as $\beta \rightarrow 1$, this component vanishes and the hidden subclusters become harder to recover.

After generating \mathbf{X} , we uniformly mask 60% of its entries and apply each matrix completion method. We then run K -means on the completed matrix and evaluate recovery of the hidden subcluster labels s . This simulation can be viewed through an effects-decomposition lens: the observed group labels act as nuisance factors, and GAME uses them to regularize group-specific variation so that the completed matrix better preserves the crossed latent subcluster geometry.

Results. Figure 2 shows that GAME most accurately recovers the hidden subclusters across small and moderate values of β , nearly matching the fully observed oracle that clusters X_{full} . In contrast, global completion methods and side-information baselines degrade earlier as the subcluster signal weakens, indicating that they preserve less of the local row geometry after completion. As $\beta \rightarrow 1$, the subcluster-specific component vanishes, the oracle performance drops, and all methods converge to similar clustering performance.

These results support the central intuition of GAME: when observed meta-categories carry low-rank structure, group-aware regularization can account for group-specific variation while preserving the crossed latent directions that define hidden subclusters.

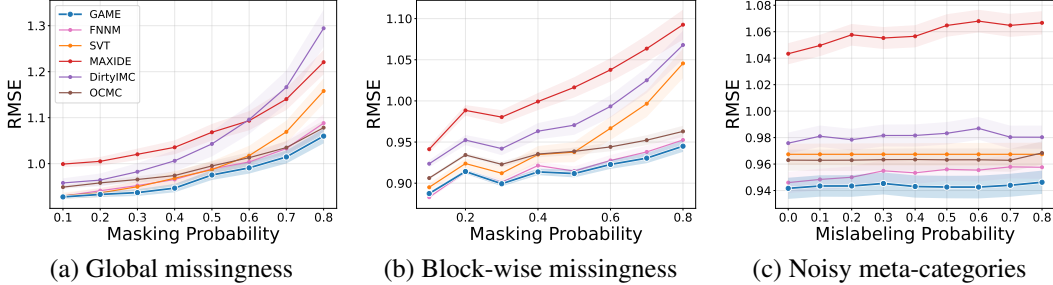


Figure 3: Test RMSE (\downarrow) on MovieLens-100k under global missingness, block-wise missingness targeting users aged 35+, and corrupted demographic metadata. GAME achieves the lowest RMSE across all three regimes. Shaded regions denote ± 1 standard error across masking realizations.

4.2 MovieLens-100k Dataset: Missingness and Meta-Category Robustness

Setup. The MovieLens-100k dataset [Harper and Konstan, 2015] contains 100,000 ratings from 943 users on 1,682 movies, together with user metadata including gender, age, occupation, and ZIP code. We use age and gender as meta-categories and omit occupation and ZIP code. We evaluate matrix completion by holding out observed ratings and reporting test

$$\text{RMSE}(\widehat{\mathbf{W}}) = \sqrt{\frac{1}{|\Omega_{\text{test}}|} \sum_{(i,j) \in \Omega_{\text{test}}} (\widehat{W}_{ij} - X_{ij})^2},$$

where Ω_{test} is the held-out set of observed ratings.

We consider three regimes. First, in the *global missingness* setting, we uniformly mask a proportion p_{global} of observed ratings. Second, in the *block-wise missingness* setting, we first hold out 10% of ratings globally, then additionally mask a proportion p_{block} of ratings from users aged 35+. This setting tests whether methods can recover ratings for a systematically under-observed subgroup by borrowing information through overlapping demographic structure.

Third, we evaluate robustness to misspecified metadata. We impose 50% global missingness and corrupt the user-level meta-categories in the training set. For each user, we randomly select either gender or age with equal probability, then corrupt the selected label with probability p_{swap} . We sweep p_{swap} from 0 to 0.8 to assess sensitivity to unreliable demographic metadata.

Results. Figure 3 shows GAME is consistently among the strongest methods across the three MovieLens settings. We omit ALS because it yields substantially weaker reconstruction performance. Under global missingness, GAME achieves the lowest RMSE across all masking probabilities and remains stable as sparsity increases. Its advantage is largest under block-wise missingness, where GAME attains the lowest RMSE across nearly all values of p_{block} and the gap widens as subgroup missingness increases. Under meta-category swapping, GAME remains stable as p_{swap} increases and continues to outperform the side-information baselines. FNNM is the strongest competing method.

Together, these results suggest that overlapping demographic structure is most useful when missingness is itself structured by subgroup. The corruption experiment further indicates that GAME does not rely blindly on metadata: noisy labels weaken the alignment between demographic groups and rating patterns, but the estimator can still borrow strength from the observed ratings and the remaining correctly specified group memberships.

4.3 Multi-label BirdSet: Downstream Classification

Setup. BirdSet [Rauch et al., 2025] is a large-scale benchmark for birdsong classification. We use the High Sierras Nevada (HSN) subset [Clapp et al., 2023], which contains 5460 focal training recordings for each of the 21 bird species, and 12,000 soundscape test recordings that may contain multiple bird species. We exclude rare species, unlabeled samples, and low-quality recordings.

Because GAME and the baselines operate on matrices, we do not apply them directly to raw audio waveforms. Instead, we convert each audio clip into a fixed-length feature vector using Mel-frequency

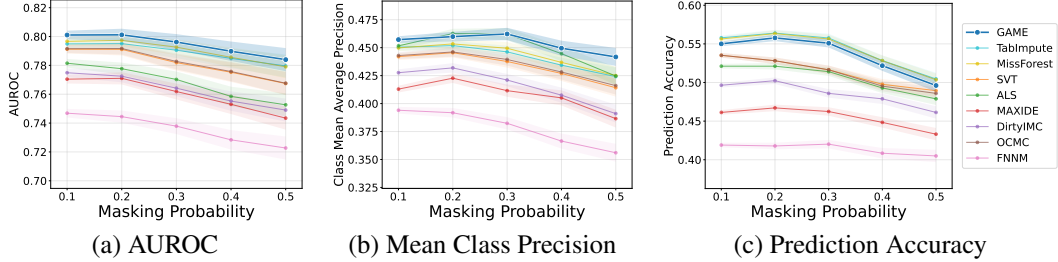


Figure 4: Downstream species-classification performance on BirdSet HSN after imputing masked MFCC features under label-structured missingness, evaluated by AUROC (\uparrow), cmAP (\uparrow), and top-1 prediction accuracy (\uparrow). GAME-completed features preserve classification signal across masking probabilities, remaining competitive or best among all methods. Shaded regions denote ± 1 standard error across masking realizations.

cepstral coefficients (MFCCs), producing a feature matrix $\mathbf{X} \in \mathbb{R}^{n \times 40}$. Rows correspond to audio clips and columns correspond to MFCC features. Here, we use bird species and recording location as meta-categorical information when applying GAME and other baselines.

We use species labels to define observed group structure for matrix completion, but the labels themselves are not imputed. We then impose structured block missingness by masking a fraction of MFCC entries among selected species. This creates a label-structured missingness pattern, corresponding to a missing-not-at-random (MNAR) setting in the imputation literature. After completing the feature matrix, we evaluate whether the imputed features preserve information useful for downstream multi-label species classification.

Results. Figure 4 evaluates whether the completed MFCC features preserve information useful for downstream multi-label species classification. For each completed feature matrix, we train a random forest classifier and report AUROC, class mean average precision (cmAP), and top-1 prediction accuracy on the multi-label soundscape test set.

GAME achieves strong downstream performance across all three metrics as the masking probability increases. It is consistently among the best methods for AUROC and cmAP, indicating that the completed features preserve species-discriminative ranking information. For top-1 prediction accuracy, GAME remains competitive, although the modern tabular imputation baselines perform slightly better at some masking levels. Overall, these results suggest that group-aware completion can preserve downstream classification signal under label-structured missingness, even when the evaluation is not based directly on reconstruction error.

4.4 Svoboda Lab Neuropixel Dataset

The Svoboda dataset [Chen et al. \[2024\]](#) consists of large-scale, simultaneous neuronal spike activity of mice performing standardized behavioral tasks (memory-guided directional licking stimulated at $t = 50$), repeated across many recording sessions and spanning prespecified brain regions (Figure 1). For a single trial, we observe a matrix $\mathbf{X} \in \mathbb{R}^{N \times T}$, where $N=50000$ is the number of neurons measured across all brain regions in the session, and $T=400$ refers to the duration of the recording. Matrix entries are 1 if the neuron spiked at time t and 0 otherwise. Figure 7 shows the structured missingness of the dataset of regions measured in 20 of the most recorded sessions. We bin the data into 10 ms windows over fixed 4-second trials, for $T = 400$, and align the trials to the stimulus ($t = 50$). We further restrict analyses to successful trial types from either “hit left” or “hit right”, keeping neurons with more than 10 spikes along the 400 timepoints, and specifically select the most populous single trial type (trial ID 0). We randomly select 20 of the most measured recording sessions and 5 of the most heavily measured brain regions across those recordings. We select recording sessions 123, 146, and 134, and within these sessions, select only regions 124 (midbrain reticular nucleus), 248 (striatum), and 258 (superior colliculus). As we observe in the region-session dynamics from PCA (Figure 8) and in the mean neuron firing rates in Figure 9, the same region can have differing temporal dynamics even when controlling for task, since here we select only from a single trial type. In this analysis, region and session latent dynamics overlap significantly, and we cannot

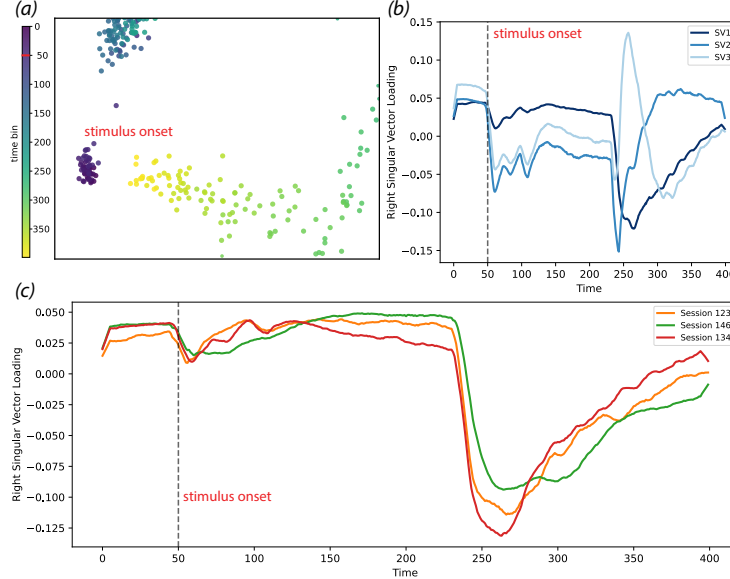


Figure 5: **GAME identifies meaningful neural dynamics while accounting for time-dependent batch effects from different recording sessions.** (a) 2D singular vectors from GAME from the striatum over time. (b) Top 3 singular vectors show clear neural dynamic response to stimulus and from the onset of mouse movement ($\sim t = 250$). (c) Temporal session-specific batch effects from GAME.

expect $V_r \perp V_s$. Generally, region dynamics are of greater interest, where sessions are treated as nuisance parameters. We still demonstrate the effectiveness of including sessions as a meta-category in our model by comparing two GAME estimators (one using both regions and sessions, the other only regions) and comparing their recovery of latent dynamics with respect to the Grassmann distance [Ye and Lim, 2016].

Briefly, if $U, V \in \mathbb{R}^{T \times k}$ have orthonormal columns spanning \mathcal{U} and \mathcal{V} , then the cosines of the principal angles are given by the singular values of $U^\top V$, $\cos(\theta_i) = \sigma_i(U^\top V)$ for $i = 1, \dots, k$, so that smaller θ_i indicate closer alignment of the two subspaces.

In particular, even though sessions are a nuisance parameter here, adding them to the GAME model can help with decontamination, since their effects may still be systematic and large, preventing region subspaces from rotating to fit session artifacts. Further, we reduce leakage, preventing sessions from corrupting regions.

Results We evaluate matrix completion when masking the striatum, a region with distinct temporal dynamics from other experimentally measured regions [Chen et al., 2024]. As shown in Figure 6, GAME consistently outperforms comparison methods in Grassmann distance, indicating more accurate recovery of latent neural dynamics. In the setting of Neuropixel data, true latent dynamics are of much greater scientific interest [Pandarinath et al., 2018, Churchland et al., 2012, Vyas et al., 2020] than the imputation of individual neuron spike trains which are noisy and highly varying [Boussard et al., 2021].

In Figure 5(a), the top two singular vectors show a shared latent dynamic learned across sessions after adjusting for session-specific effects; com-

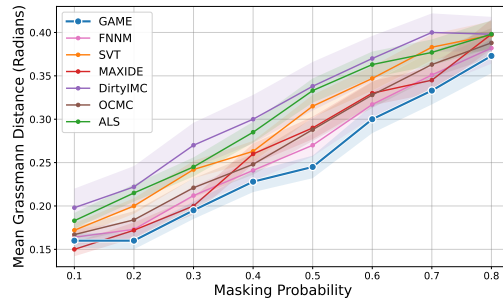


Figure 6: **Latent subspace recovery on the Svoboda Lab Neuropixels dataset**, measured by mean Grassmann distance (\downarrow) between recovered and fully observed striatal subspaces. GAME attains the lowest distance across masking probabilities, indicating best recovery of latent neural dynamics. Shaded regions denote ± 1 standard error across masking realizations.

pared with the striatum column in Figure 7 and firing rates in Figure 9, these dynamics separate pre-stimulus activity ($0 < t < 50$), pre-movement activity, and movement onset ($\sim 250 < t < 400$). Figure 5(b) further shows the top three singular vectors, revealing stimulus-locked activity near $t = 50$ and additional movement-related dynamics near $t = 250$, while Figure 5(c) shows that session-specific effects are minimal through stimulus onset but become more pronounced during movement. Together, these results recapitulate the striatal dynamics identified in [Chen et al., 2024], but do so directly from the learned decomposition without requiring extensive electrophysiological validation or domain-specific annotation.

5 Discussion

In this work, we presented Group-Aware Matrix Estimation (GAME), a convex framework for heterogeneous matrix completion that leverages overlapping meta-categorical information to promote subgroup-wise low-rank structure. We developed finite-sample theoretical guarantees for both Frobenius reconstruction error and per-category subspace recovery, showing that GAME’s statistical complexity depends on the sum of local category ranks rather than the global rank, yielding strict improvements over standard nuclear-norm regularization when subgroups exhibit distinct low-rank geometry in the tall matrix regime. We further introduced a scalable proximal-averaging optimization procedure that avoids the consensus overhead of ADMM, making GAME practical even when the number of overlapping categories is large.

The breadth of our experimental evaluation underscores GAME’s generalizability as a tool across disciplines, tasks, and data modalities. From collaborative filtering on user-movie ratings, to multi-label classification from acoustic features in ecological monitoring, to recovery of latent neural dynamics from large-scale electrophysiological recordings, GAME consistently performed competitively or best, with the largest gains appearing when subgroups carried distinct low-rank structure, and missingness was non-uniform. These results suggest that GAME is not narrowly suited to any single application domain but rather serves as a broadly applicable framework for matrix completion and latent subspace recovery wherever heterogeneous observations admit overlapping categorical structure. GAME’s ability to simultaneously reconstruct missing entries and preserve local latent geometry positions it as a practical tool for scientific and operational settings in which downstream analyses depend on faithful recovery of subgroup-specific variation.

A current limitation is that GAME’s advantages depend on the meta-categories capturing meaningful subgroup-specific low-rank structure; when metadata are weakly informative or unrelated to the missingness pattern, the estimator may offer limited improvement over global methods. The present theoretical results also rely on block-wise uniform sampling, and extending these guarantees to general sampling conditions using techniques from [Klopp, 2014] remains an important open direction. On the experimental side, future work on Neuropixels data will incorporate meta-categories for different trials and different mice, further testing GAME’s capacity to disentangle overlapping sources of neural variability. The Svoboda data in full contains 293 neural regions, 173 recording sessions, and can be further expanded to include meta-categories for different trials and different mice [Chen et al., 2024], in addition to big-data extensions to incorporate other publicly available Neuropixels data from the International Brain Laboratory [Abbott et al., 2017] and include site as a meta-category.

More broadly, the principle that regularization should reflect known categorical structure in the data, rather than imposing a single monolithic low-rank assumption, extends naturally beyond the settings studied here. Domains such as multi-omics integration [Subramanian et al., 2020], where samples span overlapping tissue types, disease subtypes, and assay platforms with block-structured missingness, and electronic health records (EHR), where clinical observations are indexed by overlapping demographic and diagnostic categories partially observed depending on site [Wells et al., 2013, Teoh et al., 2024], present immediate opportunities for group-aware estimation. By unifying scalable optimization, finite-sample theory, and empirical validation across diverse domains, GAME establishes group-aware regularization as a principled and practical paradigm for high-dimensional heterogeneous matrix estimation.

Acknowledgments

G.I.A acknowledges funding from NSF DMS-1554821. We thank Ji Xia for her help and expertise in processing the Svoboda Neuropixels data.

References

- Larry F Abbott, Dora E Angelaki, Matteo Carandini, Anne K Churchland, Yang Dan, Peter Dayan, Sophie Deneve, Ila Fiete, Surya Ganguli, Kenneth D Harris, et al. An international laboratory for systems and computational neuroscience. *Neuron*, 96(6):1213–1218, 2017.
- Andreas Argyriou, Theodoros Evgeniou, and Massimiliano Pontil. Convex multi-task feature learning. *Machine Learning*, 73(3):243–272, 2008.
- Mehdi Azabou, Krystal Xuejing Pan, Vinam Arora, Ian Jarratt Knight, Eva L Dyer, and Blake Aaron Richards. Multi-session, multi-task neural decoding from distinct cell-types and brain regions. In *The Thirteenth International Conference on Learning Representations*, 2024.
- Heinz H. Bauschke, Rafal Goebel, Yves Lucet, and Xianfu Wang. The proximal average: Basic theory. *SIAM Journal on Optimization*, 19(2):766–785, 2008. doi: 10.1137/070687542. URL <https://doi.org/10.1137/070687542>.
- Amir Beck and Marc Teboulle. A fast iterative shrinkage-thresholding algorithm for linear inverse problems. *SIAM Journal on Imaging Sciences*, 2(1):183–202, 2009. doi: 10.1137/080716542. URL <https://doi.org/10.1137/080716542>.
- Julien Boussard, Erdem Varol, Hyun Dong Lee, Nishchal Dethle, and Liam Paninski. Three-dimensional spike localization and improved motion correction for neuropixels recordings. *Advances in Neural Information Processing Systems*, 34:22095–22105, 2021.
- Stephen Boyd, Neal Parikh, Eric Chu, Borja Peleato, and Jonathan Eckstein. Distributed optimization and statistical learning via the alternating direction method of multipliers. *Foundations and Trends in Machine Learning*, 3(1):1–122, 2011.
- E. Kelly Buchanan, Ian Kinsella, Ding Zhou, Rong Zhu, Pengcheng Zhou, Felipe Gerhard, John Ferrante, Ying Ma, Sharon Kim, Mohammed Shaik, Yajie Liang, Rongwen Lu, Jacob Reimer, Paul Fahey, Taliah Muhammad, Graham Dempsey, Elizabeth Hillman, Na Ji, Andreas Tolia, and Liam Paninski. Penalized matrix decomposition for denoising, compression, and improved demixing of functional imaging data, 2018. URL <https://arxiv.org/abs/1807.06203>.
- Jian-Feng Cai, Emmanuel J. Candès, and Zuowei Shen. A singular value thresholding algorithm for matrix completion. *SIAM Journal on Optimization*, 20(4):1956–1982, 2010. doi: 10.1137/080738970. URL <https://doi.org/10.1137/080738970>.
- Emmanuel J. Candès and Yaniv Plan. Tight oracle bounds for low-rank matrix recovery from a minimal number of random measurements, 2010. URL <https://arxiv.org/abs/1001.0339>.
- Emmanuel J. Candès and Benjamin Recht. Exact matrix completion via convex optimization, 2008. URL <https://arxiv.org/abs/0805.4471>.
- Steven Cao, Percy Liang, and Gregory Valiant. One-sided matrix completion from two observations per row, 2023. URL <https://arxiv.org/abs/2306.04049>.
- Andersen Chang, Lili Zheng, and Genevera I. Allen. Low-rank covariance completion for graph quilting with applications to functional connectivity, 2024. URL <https://arxiv.org/abs/2209.08273>.
- Gengshuo Chang, Wei Zhang, and Lehan Zhang. Matrix completion with incomplete side information via orthogonal complement projection. In Aarti Singh, Maryam Fazel, Daniel Hsu, Simon Lacoste-Julien, Felix Berkenkamp, Tegan Maharaj, Kiri Wagstaff, and Jerry Zhu, editors, *Proceedings of the 42nd International Conference on Machine Learning*, volume 267 of *Proceedings of Machine Learning Research*, pages 7393–7416. PMLR, 13–19 Jul 2025. URL <https://proceedings.mlr.press/v267/chang25e.html>.
- Susu Chen, Yi Liu, Ziyue Aiden Wang, Jennifer Colonell, Liu D. Liu, Han Hou, Nai-Wen Tien, Tim Wang, Timothy Harris, Shaul Druckmann, Nuo Li, and Karel Svoboda. Brain-wide neural activity underlying memory-guided movement. *Cell*, 187(3):676–691.e16, 2024. ISSN 0092-8674. doi: <https://doi.org/10.1016/j.cell.2023.12.035>. URL <https://www.sciencedirect.com/science/article/pii/S0092867423014459>.

- Kai-Yang Chiang, Cho-Jui Hsieh, and Inderjit S Dhillon. Matrix completion with noisy side information. In C. Cortes, N. Lawrence, D. Lee, M. Sugiyama, and R. Garnett, editors, *Advances in Neural Information Processing Systems*, volume 28. Curran Associates, Inc., 2015. URL https://proceedings.neurips.cc/paper_files/paper/2015/file/0609154fa35b3194026346c9cac2a248-Paper.pdf.
- Mark M Churchland, John P Cunningham, Matthew T Kaufman, Justin D Foster, Paul Nuyujukian, Stephen I Ryu, and Krishna V Shenoy. Neural population dynamics during reaching. *Nature*, 487(7405):51–56, 2012.
- Mary Clapp, Stefan Kahl, Erik Meyer, Megan McKenna, Holger Klinck, and Gail Patricelli. A collection of fully-annotated soundscape recordings from the southern sierra nevada mountain range, January 2023. URL <https://doi.org/10.5281/zenodo.7525805>.
- Patrick L. Combettes and Jean-Christophe Pesquet. Proximal splitting methods in signal processing, 2010. URL <https://arxiv.org/abs/0912.3522>.
- Max Dabagia, Konrad P Kording, and Eva L Dyer. Comparing high-dimensional neural recordings by aligning their low-dimensional latent representations, 2022. URL <https://arxiv.org/abs/2205.08413>.
- Ehsan Elhamifar and René Vidal. Sparse subspace clustering: Algorithm, theory, and applications. *IEEE Transactions on Pattern Analysis and Machine Intelligence*, 35(11):2765–2781, 2013.
- Jacob Feitelberg, Dwaipayan Saha, Kyuseong Choi, Zaid Ahmad, Anish Agarwal, and Raaz Dwivedi. Tabimpute: Universal zero-shot imputation for tabular data, 2026. URL <https://arxiv.org/abs/2510.02625>.
- Daniel Gabay and Bertrand Mercier. A dual algorithm for the solution of nonlinear variational problems via finite element approximation. *Computers & Mathematics with Applications*, 2(1):17–40, 1976.
- Roland Glowinski and Antoinette Marrocco. Sur l’approximation, par éléments finis d’ordre un, et la résolution, par pénalisation-dualité, d’une classe de problèmes de Dirichlet non linéaires. *Revue française d’automatique, informatique, recherche opérationnelle. Analyse numérique*, 9(R2):41–76, 1975.
- F. Maxwell Harper and Joseph A. Konstan. The movielens datasets: History and context. *ACM Transactions on Interactive Intelligent Systems (TiiS)*, 5(4):19:1–19:19, December 2015. doi: 10.1145/2827872. URL <https://doi.org/10.1145/2827872>.
- Trevor Hastie, Rahul Mazumder, Jason Lee, and Reza Zadeh. Matrix completion and low-rank svd via fast alternating least squares, 2014. URL <https://arxiv.org/abs/1410.2596>.
- Prateek Jain and Inderjit S. Dhillon. Provable inductive matrix completion, 2013. URL <https://arxiv.org/abs/1306.0626>.
- Prateek Jain, Praneeth Netrapalli, and Sujay Sanghavi. Low-rank matrix completion using alternating minimization, 2012. URL <https://arxiv.org/abs/1212.0467>.
- Olga Klopp. Noisy low-rank matrix completion with general sampling distribution. *Bernoulli*, 20(1), February 2014. ISSN 1350-7265. doi: 10.3150/12-bej486. URL <http://dx.doi.org/10.3150/12-BEJ486>.
- Guangcan Liu, Zhouchen Lin, Shuicheng Yan, Ju Sun, Yong Yu, and Yi Ma. Robust recovery of subspace structures by low-rank representation. *IEEE Transactions on Pattern Analysis and Machine Intelligence*, 35(1):171–184, January 2013. ISSN 2160-9292. doi: 10.1109/tpami.2012.88. URL <http://dx.doi.org/10.1109/TPAMI.2012.88>.
- Rahul Mazumder, Trevor Hastie, and Robert Tibshirani. Spectral regularization algorithms for learning large incomplete matrices. *Journal of Machine Learning Research*, 11(80):2287–2322, 2010. URL <http://jmlr.org/papers/v11/mazumder10a.html>.

- Sahand Negahban and Martin J. Wainwright. Restricted strong convexity and weighted matrix completion: Optimal bounds with noise, 2011. URL <https://arxiv.org/abs/1009.2118>.
- Sahand N. Negahban, Pradeep Ravikumar, Martin J. Wainwright, and Bin Yu. A unified framework for high-dimensional analysis of m -estimators with decomposable regularizers. *Statistical Science*, 27(4), November 2012. ISSN 0883-4237. doi: 10.1214/12-sts400. URL <http://dx.doi.org/10.1214/12-STS400>.
- Guillaume Obozinski, Laurent Jacob, and Jean-Philippe Vert. Group lasso with overlaps: the latent group lasso approach, 2011. URL <https://arxiv.org/abs/1110.0413>.
- Chethan Pandarinath, Daniel J. O’Shea, Jasmine Collins, Rafal Jozefowicz, Sergey D. Stavisky, Jonathan C. Kao, Eric M. Trautmann, Matthew T. Kaufman, Stephen I. Ryu, Leigh R. Hochberg, Jaimie M. Henderson, Krishna V. Shenoy, L. F. Abbott, and David Sussillo. Inferring single-trial neural population dynamics using sequential auto-encoders. *Nature Methods*, 15:805–815, 2018. doi: 10.1038/s41592-018-0109-9. URL <https://doi.org/10.1038/s41592-018-0109-9>.
- Neal Parikh and Stephen Boyd. Proximal algorithms. *Foundations and Trends® in Optimization*, 1(3):127–239, 2014. ISSN 2167-3888. doi: 10.1561/2400000003. URL <http://dx.doi.org/10.1561/2400000003>.
- Arthur Pellegrino, Heike Stein, and N. Alex Cayco-Gajic. Dimensionality reduction beyond neural subspaces with slice tensor component analysis. *Nature Neuroscience*, 27(6):1199–1210, may 2024. doi: 10.1038/s41593-024-01626-2. URL <https://doi.org/10.1038/s41593-024-01626-2>. Technical Report, Open Access.
- Lukas Rauch, Raphael Schwinger, Moritz Wirth, René Heinrich, Denis Huseljic, Marek Herde, Jonas Lange, Stefan Kahl, Bernhard Sick, Sven Tomforde, and Christoph Scholz. Birdset: A large-scale dataset for audio classification in avian bioacoustics, 2025. URL <https://arxiv.org/abs/2403.10380>.
- Benjamin Recht, Maryam Fazel, and Pablo A. Parrilo. Guaranteed minimum-rank solutions of linear matrix equations via nuclear norm minimization. *SIAM Review*, 52(3):471–501, January 2010. ISSN 1095-7200. doi: 10.1137/070697835. URL <http://dx.doi.org/10.1137/070697835>.
- Daniel J. Stekhoven and Peter Bühlmann. Missforest—non-parametric missing value imputation for mixed-type data. *Bioinformatics*, 28(1):112–118, October 2011. ISSN 1367-4803. doi: 10.1093/bioinformatics/btr597. URL <http://dx.doi.org/10.1093/bioinformatics/btr597>.
- Indhupriya Subramanian, Srikant Verma, Shiva Kumar, Abhay Jere, and Krishanpal Anamika. Multi-omics data integration, interpretation, and its application. *Bioinformatics and biology insights*, 14: 1177932219899051, 2020.
- Jing Ru Teoh, Jian Dong, Xiaowei Zuo, Khin Wee Lai, Khairunnisa Hasikin, and Xiang Wu. Advancing healthcare through multimodal data fusion: a comprehensive review of techniques and applications. *PeerJ Computer Science*, 10:e2298, 2024.
- Joel A. Tropp. User-friendly tail bounds for sums of random matrices. *Found. Comput. Math.*, 12(4): 389–434, August 2012. ISSN 1615-3375.
- Saurabh Vyas, Matthew D Golub, David Sussillo, and Krishna V Shenoy. Computation through neural population dynamics. *Annual review of neuroscience*, 43(1):249–275, 2020.
- Martin J. Wainwright. *High-Dimensional Statistics: A Non-Asymptotic Viewpoint*. Cambridge Series in Statistical and Probabilistic Mathematics. Cambridge University Press, 2019.
- Jiuzhou Wang and Eric F Lock. Multiple augmented reduced rank regression for pan-cancer analysis. *Biometrics*, 80(1):ujad002, 01 2024. ISSN 0006-341X. doi: 10.1093/biomtc/ujad002. URL <https://doi.org/10.1093/biomtc/ujad002>.
- Brian J Wells, Kevin M Chagin, Amy S Nowacki, and Michael W Kattan. Strategies for handling missing data in electronic health record derived data. *Egems*, 1(3):1035, 2013.

- Alex H. Williams, Tony Hyun Kim, Forea Wang, Saurabh Vyas, Stephen I. Ryu, Krishna V. Shenoy, Mark J. Schnitzer, Tamara G. Kolda, and Surya Ganguli. Unsupervised discovery of demixed, low-dimensional neural dynamics across multiple timescales through tensor component analysis. *Neuron*, 98(6):1099–1115.e8, 2018. doi: 10.1016/j.neuron.2018.05.015. URL <https://doi.org/10.1016/j.neuron.2018.05.015>.
- Ji Xia, Yizi Zhang, Shuqi Wang, Genevera I. Allen, Liam Paninski, Cole Lincoln Hurwitz, and Kenneth D. Miller. Inpainting the neural picture: Inferring unrecorded brain area dynamics from multi-animal datasets, 2025. URL <https://arxiv.org/abs/2510.11924>.
- Miao Xu, Rong Jin, and Zhi-Hua Zhou. Speedup matrix completion with side information: Application to multi-label learning. In C.J. Burges, L. Bottou, M. Welling, Z. Ghahramani, and K.Q. Weinberger, editors, *Advances in Neural Information Processing Systems*, volume 26. Curran Associates, Inc., 2013. URL https://proceedings.neurips.cc/paper_files/paper/2013/file/e58cc5ca94270acaceed13bc82dfedf7-Paper.pdf.
- Mengyun Yang, Yaohang Li, and Jianxin Wang. Feature and nuclear norm minimization for matrix completion. *IEEE Transactions on Knowledge and Data Engineering*, 34(5):2190–2199, 2022.
- Ke Ye and Lek-Heng Lim. Schubert varieties and distances between subspaces of different dimensions. *SIAM Journal on Matrix Analysis and Applications*, 37(3):1176–1197, 2016.
- Byron M. Yu, John P. Cunningham, Gopal Santhanam, Stephen I. Ryu, Krishna V. Shenoy, and Maneesh Sahani. Gaussian-process factor analysis for low-dimensional single-trial analysis of neural population activity. *Journal of Neurophysiology*, 102(1):614–635, 2009. doi: 10.1152/jn.90941.2008. URL <https://doi.org/10.1152/jn.90941.2008>.
- Y. YU, T. WANG, and R. J. SAMWORTH. A useful variant of the davis—kahan theorem for statisticians. *Biometrika*, 102(2):315–323, 2015. ISSN 00063444. URL <http://www.jstor.org/stable/43908537>.
- Yao-Liang Yu. Better approximation and faster algorithm using the proximal average. In C.J. Burges, L. Bottou, M. Welling, Z. Ghahramani, and K.Q. Weinberger, editors, *Advances in Neural Information Processing Systems*, volume 26. Curran Associates, Inc., 2013. URL https://proceedings.neurips.cc/paper_files/paper/2013/file/49182f81e6a13cf5eaa496d51fea6406-Paper.pdf.
- Yizi Zhang, Yanchen Wang, Donato Jiménez-Benetó, Zixuan Wang, Mehdi Azabou, Blake Richards, Renee Tung, Olivier Winter, Eva Dyer, Liam Paninski, et al. Towards a "universal translator" for neural dynamics at single-cell, single-spike resolution. *Advances in Neural Information Processing Systems*, 37:80495–80521, 2024.
- Yizi Zhang, Hanrui Lyu, Cole Hurwitz, Shuqi Wang, Charles Findling, Yanchen Wang, Felix Hubert, Alexandre Pouget, Erdem Varol, and Liam Paninski. Exploiting correlations across trials and behavioral sessions to improve neural decoding. *Neuron*, 2025.

A Theory for Proximal Averaging Convergence Guarantees

A.1 Proximal Averaging Background

Definition A.1 (Proximal Operator). Let $x, z \in \mathbb{X}$, where \mathbb{X} is a real Hilbert space. We define the *proximal operator* of a function f as a mapping

$$\text{prox}_{\gamma f}(x) = \arg \min_z \frac{1}{2\gamma} \|x - z\|_2^2 + f(z).$$

A function is *simple* if it has a closed form proximal operator. Proximal operators exhibit many desirable algebraic properties that prove to be extremely useful in solving convex optimization problems. A particularly nice property of proximal operators is utilized in constructing the GAME solution. More generally, an optimization procedure known as *proximal gradient descent* is successful if the objective is separable into a convex and differentiable component f , and another convex, but not necessarily differentiable, component h [Parikh and Boyd, 2014]:

$$\arg \min_{x \in \mathbb{X}} f(x) + h(x).$$

To minimize the following general multi-term, nonsmooth convex minimization problem

$$\arg \min_{x \in \mathbb{X}} F(x) = f(x) + \bar{g}(x), \quad \text{where } \bar{g}(x) = \sum_{k=1}^K \alpha_k g_k(x) \quad (6)$$

Here, $\alpha_k \geq 0$ satisfying $\sum_{k=1}^K \alpha_k = 1$, $g_k : \mathbb{X} \rightarrow [-\infty, \infty]$ is a proper closed convex function, and $f : \mathbb{X} \rightarrow (-\infty, \infty)$ is a continuously differentiable and gradient L_f Lipschitz convex function. This is exactly the minimization problem [Yu, 2013] considered, relying on proximal averaging approximations to solve the (6).

Definition A.2 (Proximal Average, Bauschke et al. 2008 [Bauschke et al., 2008]). We define the *Proximal Average function* The Proximal Average function of $g(x) = \sum_{k=1}^K \alpha_k g_k(x)$ with parameter $\gamma > 0$ is defined by the optimization problem

$$g_\gamma(x) := \min_{y_k} \left\{ \sum_{k=1}^K \alpha_k g_k(y_k) + \frac{1}{2\gamma} \left(\sum_{k=1}^K \alpha_k \|y_k\|^2 - \|x\|^2 \right) \quad : \quad \sum_{k=1}^K \alpha_k y_k = x \right\}$$

The proximal operator of the Proximal Average function satisfies the nice property

$$\text{prox}_{g_\gamma, \gamma} = \alpha_1 \text{prox}_{g_1, \gamma} + \cdots + \alpha_N \text{prox}_{g_N, \gamma}$$

This result says that the proximal operator of g_γ with respect to the same step size γ is additive in the individual proximal operators of each g_k . The power of this formulation stems from the fact that the proximal operator of the function $\bar{g}(x)$ might not have a nice closed form equation, but each of the individual g_k 's do, allowing us to construct an approximation with convergence guarantees. With the construction of a Proximal Average, [Yu, 2013] solve (6) via the approximation

$$\arg \min_{x \in \mathbb{X}} f(x) + g_\gamma(x) \quad (7)$$

Observe that this problem is of the same form as proximal gradient descent. [Yu, 2013] makes this exact connection, plugging the approximate objective function into the updates provided in proximal gradient descent. [Yu, 2013] also provides theoretical justifications for the aforementioned algorithm, under a few assumptions.

In particular, their proposed algorithm takes the form of the Fast Iterative Shrinkage–Thresholding Algorithm (FISTA) [Beck and Teboulle, 2009] outlined in Algorithm 2, as well as a non-accelerated ISTA in Algorithm 3. The accelerated version is referred to as “accelerated proximal gradient” (PA-APG), whereas the non-accelerated counterpart is PA-PG.

Denote $\bar{L}^2 = \sum_{i=k}^K \alpha_k L_k^2$ as a convex combination of each Lipschitz constant L_k .

Algorithm 2 PA-APG [Yu, 2013].

```

1: Initialize  $x_0 = y_1, \gamma, \eta_1 = 1.$ 
2: for  $t = 1, 2, \dots$  do
3:    $z_t = y_t - \gamma \nabla \ell(y_t),$ 
4:    $x_t = \sum_k \alpha_k \cdot \text{prox}_{\gamma f_k}(z_t),$ 
5:    $\eta_{t+1} = \frac{1 + \sqrt{1 + 4\eta_t^2}}{2},$ 
6:    $y_{t+1} = x_t + \frac{\eta_t - 1}{\eta_{t+1}}(x_t - x_{t-1}).$ 
7: end for

```

Algorithm 3 PA-PG [Yu, 2013].

```

1: Initialize  $x_0, \gamma.$ 
2: for  $t = 1, 2, \dots$  do
3:    $z_t = x_{t-1} - \gamma \nabla \ell(x_{t-1}),$ 
4:    $x_t = \sum_k \alpha_k \cdot \text{prox}_{\gamma f_k}(z_t).$ 
5: end for

```

Theorem A.3 (Theorem 1 of [Yu, 2013]). *Assuming the following:*

1. Each g_i is convex and L_i -Lipschitz continuous w.r.t. the Euclidean norm.
2. Each g_i is simple.
3. f is convex with L_f -Lipschitz continuous gradient w.r.t. the Euclidean norm.

Let x_0 be the initialization of the PA-APG algorithm. Fix the accuracy $\epsilon > 0$. Under assumptions 1-3, let $\gamma = \min\{1/L_f, 2\epsilon/\bar{L}^2\}$. After at most $\sqrt{\frac{2}{\gamma\epsilon}}\|x_0 - x\|_2$ steps, the PA-APG approximation, \tilde{x} , satisfies

$$f(\tilde{x}) + \bar{g}(\tilde{x}) \leq f(x) + \bar{g}(x) + 2\epsilon.$$

The same guarantee holds for the non-accelerated Proximal Average approximation after at most $\frac{1}{2\gamma\epsilon}\|\mathbf{W}_0 - \mathbf{W}\|_F^2$ steps.

A.2 Solving GAME via Proximal Averaging

The Proximal Average algorithm [Yu, 2013] requires $\sum_{c \in \mathcal{C}} \alpha_c = 1$. This yields us our final GAME optimization problem

$$\arg \min_{\mathbf{W}} \frac{1}{2} \|\mathbf{X} - \mathbf{W}\|_F^2 + \lambda \sum_{c \in \mathcal{C}} \alpha_c \|\mathbf{D}_c \mathbf{W}\|_*, \quad (8)$$

where we define $\lambda_c := \alpha_c \lambda$ to represent proportions of regularization for each meta-category $c \in \mathcal{C}$. As discussed in the previous subsection, to leverage proximal averaging techniques for solving GAME (8), we first require $f(\mathbf{W}) := \frac{1}{2} \|\mathbf{X} - \mathbf{W}\|_F^2$ to be convex with L_f -Lipschitz continuous gradient (with respect to the Euclidean norm), and each $g_c(\mathbf{W}) := \|\mathbf{D}_c \mathbf{W}\|_*$ to be convex and L_c -Lipschitz continuous with respect to the Euclidean norm. Secondly, we require that each g_c is simple (i.e. has a defined closed-form proximal operator). We claim that the assumptions hold for our GAME formulation (8) through the following propositions, constructing an analogous theorem to A.3.

It should be noted that although [Yu, 2013] defines their results for $x \in \mathbb{R}^d$ equipped with the l_2 norm, but this is not an issue since our results extend to $\mathbf{X} \in \mathbb{R}^{n \times m}$ equipped with the Frobenius norm without loss of generality. This is because the l_2 norm and Frobenius norm coincide under vectorization, i.e. $\|\text{vec}(\mathbf{X})\|_2 = \|\mathbf{X}\|_F$, meaning the two metric spaces are isometric. Further, all technical tools used by [Yu, 2013] pertain to a real Hilbert-space domain. Hence, all Lipschitz, convexity, and proximal arguments transfer verbatim.

We recognize the GAME formulation (8) as a Proximal Average problem [Yu, 2013], where g_i 's are simple (easy to compute proximal operator). Thus, we aim to massage the objective function into a composition of simple functions, but this formulation appears to be complex due to the penalties that depend on slices of \mathbf{W} that are not disjoint (i.e. there can exist $c, c' \in \mathcal{C}$ such that $c \cap c' \neq \emptyset$). Recall that \mathbf{W}_c is the row-wise "slice" of \mathbf{W} that corresponds to the c meta-category block.

The key observation to make at this stage is that $\mathbf{D}_c \mathbf{D}_c^\top = \mathbf{I}$, i.e. \mathbf{D}_c is semi-orthogonal. Using Table 10.1 from [Combettes and Pesquet, 2010], we may rewrite the proximal operator of g_c in terms of linear operations of \mathbf{D}_c and the proximal operator of the nuclear-norm, given in Proposition A.4.

Proposition A.4 (Table 10.1 of [Combettes and Pesquet, 2010]). *Define $g_c(\mathbf{W}) := \|\mathbf{D}_c \mathbf{W}\|_*$. Then,*

$$\text{prox}_{g_c}(\mathbf{A}) = \text{prox}_{\|\mathbf{D}_c \mathbf{A}\|_*}(\mathbf{A}) = \mathbf{A} - \mathbf{D}_c^\top (\mathbf{D}_c \mathbf{A} - \text{prox}_{\|\cdot\|_*}(\mathbf{D}_c \mathbf{A}))$$

From Proposition A.4, we see the nuclear-norm having a simple proximal operator is sufficient for g_c to have a simple proximal operator. The closed form proximal operator of the nuclear-norm is a well established fact [Parikh and Boyd, 2014].

Proposition A.5 (nuclear-norm Proximal Operator [Parikh and Boyd, 2014] Section 6.7.3). *Let $\lambda > 0$ and let $\mathbf{Y} \in \mathbb{R}^{m \times n}$ have the singular value decomposition of rank r*

$$\mathbf{Y} = \mathbf{U} \mathbf{\Sigma} \mathbf{V}^\top, \quad \mathbf{\Sigma} = \text{diag}(\sigma_1, \dots, \sigma_r), \quad \sigma_1 \geq \dots \geq \sigma_r > 0.$$

Then the proximal operator of the nuclear-norm,

$$\text{prox}_{\lambda \|\cdot\|_*}(\mathbf{Y}) := \arg \min_{\mathbf{X} \in \mathbb{R}^{m \times n}} \left\{ \frac{1}{2} \|\mathbf{X} - \mathbf{Y}\|_F^2 + \lambda \|\mathbf{X}\|_* \right\},$$

is given by singular value soft-thresholding:

$$\text{prox}_{\lambda \|\cdot\|_*}(\mathbf{Y}) = \mathbf{U} \text{diag}((\sigma_i - \lambda)_+) \mathbf{V}^\top,$$

where $(t)_+ := \max\{t, 0\}$ is the positive part applied entrywise to the singular values.

The following series of propositions demonstrate that assumptions made by [Yu, 2013] (found in Theorem A.3 to establish convergence guarantees) are met by the GAME estimator.

Proposition A.6. *Let $\mathbf{X} \in \mathbb{R}^{n \times m}$ be fixed and let $\mathbf{M} \in \{0, 1\}^{n \times m}$ be a binary mask encoding the observed entries, i.e. $\mathbf{M}_{ij} = 1$ if (i, j) is observed and $\mathbf{M}_{ij} = 0$ otherwise. Define the orthogonal projection $\mathcal{P}_\Omega : \mathbb{R}^{n \times m} \rightarrow \mathbb{R}^{n \times m}$ by*

$$\mathcal{P}_\Omega(\mathbf{Z}) := \mathbf{M} \odot \mathbf{Z},$$

where \odot denotes the Hadamard (entrywise) product. Consider the function

$$f(\mathbf{W}) := \frac{1}{2} \|\mathcal{P}_\Omega(\mathbf{X} - \mathbf{W})\|_F^2, \quad \mathbf{W} \in \mathbb{R}^{n \times m}.$$

Then f is convex and differentiable, with gradient

$$\nabla f(\mathbf{W}) = \mathcal{P}_\Omega(\mathbf{W} - \mathbf{X}) = \mathbf{M} \odot (\mathbf{W} - \mathbf{X}).$$

Moreover, ∇f is L_f -Lipschitz continuous with respect to the Frobenius norm with constant $L_f = 1$, that is, for all $\mathbf{W}_1, \mathbf{W}_2 \in \mathbb{R}^{n \times m}$,

$$\begin{aligned} \|\nabla f(\mathbf{W}_1) - \nabla f(\mathbf{W}_2)\|_F &\leq L_f \|\mathbf{W}_1 - \mathbf{W}_2\|_F \\ &= \|\mathbf{W}_1 - \mathbf{W}_2\|_F. \end{aligned}$$

Proof. We first rewrite f using the definition of \mathcal{P}_Ω :

$$f(\mathbf{W}) = \frac{1}{2} \|\mathcal{P}_\Omega(\mathbf{X} - \mathbf{W})\|_F^2 = \frac{1}{2} \sum_{i,j} (\mathbf{M}_{ij} (\mathbf{X}_{ij} - \mathbf{W}_{ij}))^2.$$

Since each term $\frac{1}{2} (\mathbf{M}_{ij} (\mathbf{X}_{ij} - \mathbf{W}_{ij}))^2$ is a convex function of \mathbf{W}_{ij} (a nonnegative scalar multiple of a quadratic), and f is a finite sum of convex functions, f is convex.

Next, f is differentiable, and we can compute its gradient entrywise. For each (i, j) ,

$$f(\mathbf{W}) = \frac{1}{2} \sum_{i,j} \mathbf{M}_{ij}^2 (\mathbf{W}_{ij} - \mathbf{X}_{ij})^2 = \frac{1}{2} \sum_{i,j} \mathbf{M}_{ij} (\mathbf{W}_{ij} - \mathbf{X}_{ij})^2,$$

since $\mathbf{M}_{ij}^2 = \mathbf{M}_{ij}$ for $\mathbf{M}_{ij} \in \{0, 1\}$. Differentiating with respect to \mathbf{W}_{ij} ,

$$\frac{\partial f}{\partial \mathbf{W}_{ij}} = \mathbf{M}_{ij} (\mathbf{W}_{ij} - \mathbf{X}_{ij}).$$

Thus the gradient matrix has entries

$$[\nabla f(\mathbf{W})]_{ij} = \mathbf{M}_{ij}(\mathbf{W}_{ij} - \mathbf{X}_{ij}),$$

which we can write compactly as

$$\nabla f(\mathbf{W}) = \mathbf{M} \odot (\mathbf{W} - \mathbf{X}) = \mathcal{P}_\Omega(\mathbf{W} - \mathbf{X}).$$

It remains to show that ∇f is 1-Lipschitz with respect to the Frobenius norm. Let $\mathbf{W}_1, \mathbf{W}_2 \in \mathbb{R}^{n \times m}$. Then

$$\begin{aligned} \nabla f(\mathbf{W}_1) - \nabla f(\mathbf{W}_2) &= \mathcal{P}_\Omega(\mathbf{W}_1 - \mathbf{X}) - \mathcal{P}_\Omega(\mathbf{W}_2 - \mathbf{X}) \\ &= \mathcal{P}_\Omega(\mathbf{W}_1 - \mathbf{W}_2) \\ &= \mathbf{M} \odot (\mathbf{W}_1 - \mathbf{W}_2). \end{aligned}$$

Therefore,

$$\begin{aligned} \|\nabla f(\mathbf{W}_1) - \nabla f(\mathbf{W}_2)\|_F^2 &= \|\mathbf{M} \odot (\mathbf{W}_1 - \mathbf{W}_2)\|_F^2 \\ &= \sum_{i,j} (\mathbf{M}_{ij}(\mathbf{W}_1 - \mathbf{W}_2)_{ij})^2 \\ &\leq \sum_{i,j} ((\mathbf{W}_1 - \mathbf{W}_2)_{ij})^2 \\ &= \|\mathbf{W}_1 - \mathbf{W}_2\|_F^2, \end{aligned}$$

where the inequality uses $\mathbf{M}_{ij} \in \{0, 1\}$, so $\mathbf{M}_{ij}^2 \leq 1$ entrywise. Taking square roots yields

$$\|\nabla f(\mathbf{W}_1) - \nabla f(\mathbf{W}_2)\|_F \leq \|\mathbf{W}_1 - \mathbf{W}_2\|_F,$$

showing that ∇f is 1-Lipschitz with respect to the Frobenius norm. This proves the claim with $L_f = 1$. \square

Proposition A.7. $g_c(\mathbf{W}) = \|\mathbf{D}_c \mathbf{W}\|_*$ is Lipschitz continuous with respect to the Frobenius norm on $\mathbb{R}^{n \times m}$ with Lipschitz constant

$$L_c = \sqrt{r} \|\mathbf{D}_c\|_{\text{op}}, \quad r := \min\{\ell, m\}.$$

That is, for all $\mathbf{W}_1, \mathbf{W}_2 \in \mathbb{R}^{n \times m}$,

$$|g_c(\mathbf{W}_1) - g_c(\mathbf{W}_2)| \leq L_c \|\mathbf{W}_1 - \mathbf{W}_2\|_F.$$

Proof. We first show that the nuclear-norm is \sqrt{r} -Lipschitz with respect to the Frobenius norm, where $r = \min\{m, n\}$. Let $\mathbf{A}, \mathbf{B} \in \mathbb{R}^{m \times n}$ and let $\sigma_1(\mathbf{A}) \geq \dots \geq \sigma_r(\mathbf{A})$ and $\sigma_1(\mathbf{B}) \geq \dots \geq \sigma_r(\mathbf{B})$ denote their singular values. Then

$$\begin{aligned} \left| \|\mathbf{A}\|_* - \|\mathbf{B}\|_* \right| &= \left| \sum_{j=1}^r \sigma_j(\mathbf{A}) - \sum_{j=1}^r \sigma_j(\mathbf{B}) \right| \\ &= \left| \sum_{j=1}^r (\sigma_j(\mathbf{A}) - \sigma_j(\mathbf{B})) \right| \\ &\leq \left(\sum_{j=1}^r 1^2 \right)^{1/2} \left(\sum_{j=1}^r (\sigma_j(\mathbf{A}) - \sigma_j(\mathbf{B}))^2 \right)^{1/2} \quad (\text{Cauchy-Schwarz}) \\ &= \sqrt{r} \left(\sum_{j=1}^r (\sigma_j(\mathbf{A}) - \sigma_j(\mathbf{B}))^2 \right)^{1/2}. \end{aligned}$$

By the Hoffman–Wielandt inequality for singular values,

$$\sum_{j=1}^r (\sigma_j(\mathbf{A}) - \sigma_j(\mathbf{B}))^2 \leq \|\mathbf{A} - \mathbf{B}\|_F^2,$$

so we obtain

$$|\|\mathbf{A}\|_* - \|\mathbf{B}\|_*| \leq \sqrt{r} \|\mathbf{A} - \mathbf{B}\|_F.$$

This shows that the nuclear-norm is \sqrt{r} -Lipschitz with respect to the Frobenius norm.

Now apply this with $\mathbf{A} = D_i \mathbf{W}_1$ and $\mathbf{B} = D_i \mathbf{W}_2$ for arbitrary $\mathbf{W}_1, \mathbf{W}_2 \in \mathbb{R}^{n \times m}$. We obtain

$$\begin{aligned} |g_i(\mathbf{W}_1) - g_i(\mathbf{W}_2)| &= |\|D_i \mathbf{W}_1\|_* - \|D_i \mathbf{W}_2\|_*| \\ &\leq \sqrt{r} \|D_i \mathbf{W}_1 - D_i \mathbf{W}_2\|_F \\ &= \sqrt{r} \|D_i(\mathbf{W}_1 - \mathbf{W}_2)\|_F \\ &\leq \sqrt{r} \|D_i\|_{\text{op}} \|\mathbf{W}_1 - \mathbf{W}_2\|_F, \end{aligned}$$

where in the last line we used submultiplicativity of the operator norm. Thus g_i is Lipschitz with constant $L_i = \sqrt{r} \|D_i\|_{\text{op}}$, as claimed. \square

We use the abbreviation $\overline{L^2} := \sum_{c \in \mathcal{C}} \lambda_c L_c^2 = \sum_{c \in \mathcal{C}} \lambda_c r \|D_c\|_{\text{op}}^2$ in the following theorem, and observe that $L_f = 1$ from the previous lemmas.

Theorem A.8 (Theorem 1 of [Yu, 2013]). *Let \mathbf{W}_0 be the initialization of the PA-APG algorithm. Fix the accuracy $\epsilon > 0$. Let $\gamma = \min\{1, 2\epsilon/\overline{L^2}\}$. After at most $k = \sqrt{\frac{2}{\gamma\epsilon}} \|\mathbf{W}_0 - \widehat{\mathbf{W}}\|_F^2$ steps, the PA-APG approximation, $\widetilde{\mathbf{W}}_k$, satisfies*

$$f(\widetilde{\mathbf{W}}_k) + \bar{g}(\widetilde{\mathbf{W}}_k) \leq f(\widehat{\mathbf{W}}) + \bar{g}(\widehat{\mathbf{W}}) + 2\epsilon.$$

B Theory for Group-Aware Matrix Estimation with Overlapping Meta-Categories

In developing theoretical results for GAME, we follow the matrix completion proof techniques of [Negahban and Wainwright, 2011, Negahban et al., 2012], who develop arguments based on restricted strong convexity (RSC). We adopt their uniform-sampling formulation, which is the most common setting for noisy matrix completion and yields the cleanest statements. The rowspace-recovery formulation is motivated by global matrix completion results provided by [Cao et al., 2023].

We study the restricted GAME estimator

$$\widehat{\mathbf{W}} \in \arg \min_{\mathbf{W} \in \mathbb{R}^{n \times m}} \frac{1}{2} \|\mathcal{P}_\Omega(\mathbf{X} - \mathbf{W})\|_F^2 + \sum_{c \in \mathcal{C}} \lambda_c \|\mathbf{W}_c\|_* \quad \text{s.t.} \quad \|\mathbf{W}\|_\infty \leq \frac{\alpha^*}{\sqrt{nm}}, \quad (9)$$

under the observation model $\mathbf{X} = \mathbf{W}^* + \mathbf{E}$, where \mathbf{E} has independent mean-zero entries with subexponential moment growth (Assumption B.1 below) and $\Omega \subset [n] \times [m]$ is a uniformly i.i.d. sampled multiset of N entries (sampling model detailed in Section B.1). For each meta-category $c \in \mathcal{C}$, $\mathbf{W}_c := \mathbf{W}[I_c, :]$ $\in \mathbb{R}^{n_c \times m}$ with $n_c := |I_c|$, $d_c := n_c + m$, $r_c := \text{rank}(\mathbf{W}_c^*)$. The constant α^* controls spikiness (Assumption B.2 below).

Relative to [Negahban and Wainwright, 2011], we study the regularizer as a sum of nuclear-norms over (potentially overlapping) row blocks rather than a single nuclear-norm, while the loss remains a standard squared-error on observed entries. Our analysis (a) re-derives a per-group decomposability inequality on top of the collection \mathcal{C} , (b) splits the noise inner product via row-multiplicity weights so that each piece can be controlled by a per-group spectral bound, and (c) applies N-W's RSC inequality [Negahban and Wainwright, 2011, Thm. 1] per row block, exploiting the natural per-block decomposition of uniform samples to get block-aware rates.

B.1 Notation, sampling model, and combinatorics of the overlap

We use $\langle \mathbf{A}, \mathbf{B} \rangle = \text{tr}(\mathbf{A}^\top \mathbf{B})$. For a matrix $\mathbf{A} \in \mathbb{R}^{n \times m}$ and $c \in \mathcal{C}$, $\mathbf{A}_c = \mathbf{A}[I_c, :]$. The sampling operator $\mathcal{P}_\Omega : \mathbb{R}^{n \times m} \rightarrow \mathbb{R}^{n \times m}$ zeros out entries outside Ω .

Uniform sampling. The indices (i_t, j_t) , $t = 1, \dots, N$, are drawn i.i.d. uniformly from $[n] \times [m]$, and $\Omega := \{(i_t, j_t)\}_{t=1}^N$ (multiset). For any matrix $\mathbf{A} \in \mathbb{R}^{n \times m}$,

$$\mathbb{E} \|\mathcal{P}_\Omega(\mathbf{A})\|_F^2 = \sum_{t=1}^N \mathbb{E}[A_{i_t j_t}^2] = \sum_{t=1}^N \sum_{i,j} A_{ij}^2 \mathbb{P}[(i_t, j_t) = (i, j)] = \frac{N}{nm} \|\mathbf{A}\|_F^2. \quad (10)$$

Per-block sample counts. Although the sampling is global, the analysis decomposes per meta-category through the random per-block sample count

$$N_c := |\Omega \cap (I_c \times [m])|.$$

Under uniform sampling, each sample (i_t, j_t) independently lies in $I_c \times [m]$ with probability n_c/n (the marginal probability that $i_t \in I_c$). Hence each N_c is marginally distributed as $\text{Binomial}(N, n_c/n)$ with $\mathbb{E}N_c = N n_c/n$. When groups overlap, the joint distribution of $\{N_c\}_{c \in \mathcal{C}}$ is *not* independent across c : a sample with $i_t \in I_c \cap I_{c'}$ simultaneously contributes to N_c and $N_{c'}$, so N_c and $N_{c'}$ are positively correlated. We do not need joint independence, only the marginal concentration of each N_c (which holds by Chernoff bound for binomials). A union bound over $c \in \mathcal{C}$ then gives simultaneous control:

$$\Pr[|N_c - \mathbb{E}N_c| \geq \eta \mathbb{E}N_c \text{ for some } c \in \mathcal{C}] \leq 2|\mathcal{C}| \exp\left(-\frac{\eta^2 N n_{\min}}{3n}\right), \quad (11)$$

where $n_{\min} := \min_c n_c$. So with high probability,

$$N_c \in [(1 - \eta) N n_c/n, (1 + \eta) N n_c/n] \quad \forall c \in \mathcal{C} \quad (12)$$

provided $N n_{\min}/n \gtrsim \log |\mathcal{C}|/\eta^2$, a mild condition implied by the matrix-completion sample regime $N \gtrsim (n+m) \log(n+m)$ when $n_{\min} \gtrsim \log |\mathcal{C}|$. Throughout the analysis we treat N_c as deterministic, equal to $N n_c/n$ up to constant factors, on the high-probability event (12).

Fix any single $c \in \mathcal{C}$ and condition on the realization of $N_c = k$. By the uniformity of i_t on $[n]$, the conditional distribution of i_t given $i_t \in I_c$ is uniform on I_c ; combined with the independence of j_t (uniform on $[m]$), the k samples that fell in $I_c \times [m]$ are i.i.d. uniform on $I_c \times [m]$. This is a per-block statement and holds regardless of whether the cover overlaps, i.e. it does not require independence of N_c across c . Each per-block lemma below (spectral bound, RSC) is established by conditioning on a single N_c at a time, then taking a union bound over c .

Following [Negahban and Wainwright, 2011], we also introduce the rescaled observation operator $\mathcal{X}_n : \mathbb{R}^{n \times m} \rightarrow \mathbb{R}^N$ defined by $[\mathcal{X}_n(\mathbf{A})]_t = \langle \mathbf{X}^{(t)}, \mathbf{A} \rangle$ where $\mathbf{X}^{(t)} = \sqrt{nm} \varepsilon_t \mathbf{e}_{i_t} \mathbf{e}_{j_t}^\top$. The deterministic identity

$$\|\mathcal{X}_n(\mathbf{A})\|_2^2 = nm \|\mathcal{P}_\Omega(\mathbf{A})\|_F^2 \quad \forall \mathbf{A} \in \mathbb{R}^{n \times m} \quad (13)$$

links the two formulations.

Row multiplicity. For each row $i \in [n]$, define

$$\kappa(i) := |\{c \in \mathcal{C} : i \in I_c\}|, \quad \kappa_{\max} := \max_{i \in [n]} \kappa(i), \quad \kappa_{\min} := \min_{i \in [n]} \kappa(i).$$

We require $\kappa_{\min} \geq 1$ (every row appears in at least one meta-category, otherwise the row is unidentifiable). The ratio $\kappa_{\max}^2/\kappa_{\min}^3$ will measure the price of overlap in our main theorem.

Model subspaces. For each $c \in \mathcal{C}$, let $\mathbf{W}_c^* = \mathbf{U}_c \mathbf{D}_c \mathbf{V}_c^\top$ be the thin SVD with $\mathbf{U}_c \in \mathbb{R}^{n_c \times r_c}$, $\mathbf{V}_c \in \mathbb{R}^{m \times r_c}$, and let $\mathcal{U}_c \subset \mathbb{R}^{n_c}$, $\mathcal{V}_c \subset \mathbb{R}^m$ be the column/row spaces of \mathbf{W}_c^* . Define projections

$$\mathcal{P}_{\mathcal{M}_c^\perp}(\mathbf{B}) := \mathbf{P}_{\mathcal{U}_c^\perp} \mathbf{B} \mathbf{P}_{\mathcal{V}_c^\perp}, \quad \mathcal{P}_{\mathcal{M}_c}(\mathbf{B}) := \mathbf{B} - \mathcal{P}_{\mathcal{M}_c^\perp}(\mathbf{B}).$$

We define these operators since the GAME model is in the form of an M-estimator (cf. [Negahban et al., 2012, Sec. 2]). We make the following observations:

- (D1) $\text{rank}(\mathcal{P}_{\mathcal{M}_c}(\mathbf{B})) \leq 2r_c$ for all \mathbf{B} , and the singular vectors of $\mathcal{P}_{\mathcal{M}_c}(\mathbf{B})$ are orthogonal to those of \mathbf{W}_c^* .
- (D2) (Decomposability of nuclear-norm.) Due to orthogonality,

$$\|\mathbf{W}_c^* + \mathcal{P}_{\mathcal{M}_c}(\mathbf{B})\|_* = \|\mathbf{W}_c^*\|_* + \|\mathcal{P}_{\mathcal{M}_c}(\mathbf{B})\|_*.$$

The decomposability will be critical in the proof of our main theorem, when we show that the GAME error Δ_c is constrained to a low-rank cone.

B.2 Assumptions

Assumption B.1 (Subexponential Noise). The entries E_{ij} are independent, mean zero, and *subexponential* with parameters (σ, R) : there exist constants $\sigma, R > 0$ such that

$$\mathbb{E}[E_{ij}^p] \leq \frac{p!}{2} R^{p-2} \sigma^2 \quad \text{for every integer } p \geq 2.$$

We use this formulation of subexponential distributions as found in [Tropp, 2012]. Up to universal constants of (σ, R) , this is the same as Definiton 2.7 [Wainwright, 2019], $\mathbb{E} \exp(tE_{ij}) \leq \exp(\sigma^2 t^2/2)$ for $|t| \leq 1/R$, with σ^2 playing the role of variance proxy and R the subexponential scale.

Assumption B.2 (Spikiness). There is a constant $\alpha^* \geq 1$ such that $\sqrt{nm} \|\mathbf{W}^*\|_\infty \leq \alpha^* \|\mathbf{W}^*\|_F$, i.e., the spikiness ratio $\alpha_{\text{sp}}(\mathbf{W}^*) := \sqrt{nm} \|\mathbf{W}^*\|_\infty / \|\mathbf{W}^*\|_F \leq \alpha^*$. In addition, the optimization in (9) is restricted to matrices \mathbf{W} with $\|\mathbf{W}\|_\infty \leq \alpha^* / \sqrt{nm}$, which is consistent with \mathbf{W}^* being feasible after WLOG rescaling so that $\|\mathbf{W}^*\|_F \leq 1$.

Assumption B.3 (Cover). $\bigcup_{c \in \mathcal{C}} I_c = [n]$, i.e. $\kappa_{\min} \geq 1$.

B.3 Lemmas

Decomposability of the GAME regularizer A regularizer of the form $\Phi(\mathbf{W}) = \sum_c \lambda_c \|\mathbf{W}_c\|_*$ is not decomposable in the sense of [Negahban and Wainwright, 2011] as a single norm, in particular, distinct groups $c \neq c'$ with $I_c \cap I_{c'} \neq \emptyset$ couple. Nonetheless we have the following per-group decomposability, which is sufficient for our analysis.

Lemma B.1 (Per-Group Decomposability). *For every $\mathbf{B} \in \mathbb{R}^{n \times m}$ and every $c \in \mathcal{C}$,*

$$\|\mathbf{W}_c^* + \mathbf{B}_c\|_* \geq \|\mathbf{W}_c^*\|_* + \|\mathcal{P}_{\mathcal{M}_c^\perp}(\mathbf{B}_c)\|_* - \|\mathcal{P}_{\mathcal{M}_c}(\mathbf{B}_c)\|_*.$$

Proof. By (D2) and triangle inequality, writing $\mathbf{W}_c^* + \mathbf{B}_c = [\mathbf{W}_c^* + \mathcal{P}_{\mathcal{M}_c^\perp}(\mathbf{B}_c)] + \mathcal{P}_{\mathcal{M}_c}(\mathbf{B}_c)$:

$$\begin{aligned} \|\mathbf{W}_c^* + \mathbf{B}_c\|_* &\geq \|\mathbf{W}_c^* + \mathcal{P}_{\mathcal{M}_c^\perp}(\mathbf{B}_c)\|_* - \|\mathcal{P}_{\mathcal{M}_c}(\mathbf{B}_c)\|_* \\ &= \|\mathbf{W}_c^*\|_* + \|\mathcal{P}_{\mathcal{M}_c^\perp}(\mathbf{B}_c)\|_* - \|\mathcal{P}_{\mathcal{M}_c}(\mathbf{B}_c)\|_*. \quad \square \end{aligned}$$

Splitting the noise term over overlapping groups The single technical observation that handles the overlap is a row-multiplicity reweighting that distributes any matrix inner product over the meta-categories.

Lemma B.2 (Row-Multiplicity Split). *Under Assumption B.3, for any $\mathbf{A}, \mathbf{B} \in \mathbb{R}^{n \times m}$, define for each $c \in \mathcal{C}$ the matrix $\tilde{\mathbf{A}}^{(c)} \in \mathbb{R}^{n_c \times m}$ by $[\tilde{\mathbf{A}}^{(c)}]_{i,j} = A_{ij}/\kappa(i)$ for $i \in I_c, j \in [m]$. Then*

$$\langle \mathbf{A}, \mathbf{B} \rangle = \sum_{c \in \mathcal{C}} \langle \tilde{\mathbf{A}}^{(c)}, \mathbf{B}_c \rangle \leq \sum_{c \in \mathcal{C}} \|\tilde{\mathbf{A}}^{(c)}\|_{op} \|\mathbf{B}_c\|_*.$$

Proof. By the cover assumption, $\sum_{c:i \in I_c} 1 = \kappa(i) \geq 1$ for every i , so

$$\langle \mathbf{A}, \mathbf{B} \rangle = \sum_{i,j} A_{ij} B_{ij} = \sum_{i,j} \frac{A_{ij}}{\kappa(i)} \sum_{c:i \in I_c} B_{ij} = \sum_c \sum_{i \in I_c, j} \frac{A_{ij}}{\kappa(i)} B_{ij} = \sum_c \langle \tilde{\mathbf{A}}^{(c)}, \mathbf{B}_c \rangle.$$

The inequality is trace duality between $\|\cdot\|_{op}$ and $\|\cdot\|_*$. □

Remark B.4. Here, the weights $1/\kappa(i)$ account for overcounting induced by overlap.

Deterministic optimality inequality

Lemma B.3 (Frobenius Inequality). *Let $\widehat{\mathbf{W}}$ be any minimizer of the GAME objective (9), and let $\Delta := \widehat{\mathbf{W}} - \mathbf{W}^*$. Then*

$$\frac{1}{2} \|\mathcal{P}_\Omega(\Delta)\|_F^2 \leq \langle \mathcal{P}_\Omega(\mathbf{E}), \Delta \rangle + \sum_{c \in \mathcal{C}} \lambda_c (\|\mathbf{W}_c^*\|_* - \|\mathbf{W}_c^* + \Delta_c\|_*). \quad (14)$$

Proof. By optimality of $\widehat{\mathbf{W}}$ in (9), and feasibility of \mathbf{W}^* :

$$\frac{1}{2} \|\mathcal{P}_\Omega(\widehat{\mathbf{W}} - \mathbf{X})\|_F^2 + \sum_{c \in \mathcal{C}} \lambda_c \|\widehat{\mathbf{W}}_c\|_* \leq \frac{1}{2} \|\mathcal{P}_\Omega(\mathbf{W}^* - \mathbf{X})\|_F^2 + \sum_{c \in \mathcal{C}} \lambda_c \|\mathbf{W}_c^*\|_*.$$

Substituting $\mathbf{X} = \mathbf{W}^* + \mathbf{E}$ and $\widehat{\mathbf{W}} = \mathbf{W}^* + \Delta$, so $\widehat{\mathbf{W}} - \mathbf{X} = \Delta - \mathbf{E}$ and $\widehat{\mathbf{W}}_c = \mathbf{W}_c^* + \Delta_c$,

$$\frac{1}{2} \|\mathcal{P}_\Omega(\Delta - \mathbf{E})\|_F^2 + \sum_{c \in \mathcal{C}} \lambda_c \|\mathbf{W}_c^* + \Delta_c\|_* \leq \frac{1}{2} \|\mathcal{P}_\Omega(\mathbf{E})\|_F^2 + \sum_{c \in \mathcal{C}} \lambda_c \|\mathbf{W}_c^*\|_*.$$

Expanding the squared Frobenius norm via $\|\mathbf{A} - \mathbf{B}\|_F^2 = \|\mathbf{A}\|_F^2 + \|\mathbf{B}\|_F^2 - 2\langle \mathbf{A}, \mathbf{B} \rangle$,

$$\frac{1}{2} \left[\|\mathcal{P}_\Omega(\Delta)\|_F^2 + \|\mathcal{P}_\Omega(\mathbf{E})\|_F^2 - 2\langle \mathcal{P}_\Omega(\Delta), \mathcal{P}_\Omega(\mathbf{E}) \rangle \right] + \sum_{c \in \mathcal{C}} \lambda_c \|\mathbf{W}_c^* + \Delta_c\|_* \leq \frac{1}{2} \|\mathcal{P}_\Omega(\mathbf{E})\|_F^2 + \sum_{c \in \mathcal{C}} \lambda_c \|\mathbf{W}_c^*\|_*.$$

The $\frac{1}{2} \|\mathcal{P}_\Omega(\mathbf{E})\|_F^2$ terms cancel on both sides. Using $\langle \mathcal{P}_\Omega(\Delta), \mathcal{P}_\Omega(\mathbf{E}) \rangle = \langle \Delta, \mathcal{P}_\Omega(\mathbf{E}) \rangle$ (the projection \mathcal{P}_Ω is self-adjoint and idempotent on entries) and rearranging,

$$\frac{1}{2} \|\mathcal{P}_\Omega(\Delta)\|_F^2 \leq \langle \mathcal{P}_\Omega(\mathbf{E}), \Delta \rangle + \sum_{c \in \mathcal{C}} \lambda_c (\|\mathbf{W}_c^*\|_* - \|\mathbf{W}_c^* + \Delta_c\|_*).$$

□

Applying Lemma B.2 to $\mathbf{A} = \mathcal{P}_\Omega(\mathbf{E})$ and $\mathbf{B} = \Delta$, the noise inner product splits as $\langle \mathcal{P}_\Omega(\mathbf{E}), \Delta \rangle = \sum_c \langle \widetilde{\mathbf{E}}^{(c)}, \Delta_c \rangle \leq \sum_c \|\widetilde{\mathbf{E}}^{(c)}\|_{op} \|\Delta_c\|_*$, where $\widetilde{\mathbf{E}}^{(c)} \in \mathbb{R}^{n_c \times m}$ has entries $E_{ij}/\kappa(i)$ for $(i, j) \in \Omega \cap (I_c \times [m])$ and zero elsewhere.

Lemma B.4 (Group Cone Constraint). *If*

$$\lambda_c \geq 2 \|\widetilde{\mathbf{E}}^{(c)}\|_{op} \quad \forall c \in \mathcal{C}, \quad (15)$$

then

$$\sum_{c \in \mathcal{C}} \lambda_c \|\mathcal{P}_{\mathcal{M}_c^\perp}(\Delta_c)\|_* \leq 3 \sum_{c \in \mathcal{C}} \lambda_c \|\mathcal{P}_{\mathcal{M}_c}(\Delta_c)\|_*, \quad (16)$$

and

$$\frac{1}{2} \|\mathcal{P}_\Omega(\Delta)\|_F^2 \leq \frac{3}{2} \sum_{c \in \mathcal{C}} \lambda_c \|\mathcal{P}_{\mathcal{M}_c}(\Delta_c)\|_*. \quad (17)$$

Proof. Combine (14) with Lemmas B.1 and B.2:

$$\begin{aligned} \frac{1}{2} \|\mathcal{P}_\Omega(\Delta)\|_F^2 &\leq \sum_c \|\widetilde{\mathbf{E}}^{(c)}\|_{op} (\|\mathcal{P}_{\mathcal{M}_c}(\Delta_c)\|_* + \|\mathcal{P}_{\mathcal{M}_c^\perp}(\Delta_c)\|_*) \\ &\quad + \sum_c \lambda_c (\|\mathcal{P}_{\mathcal{M}_c}(\Delta_c)\|_* - \|\mathcal{P}_{\mathcal{M}_c^\perp}(\Delta_c)\|_*) \\ &\leq \sum_c \left[\frac{3\lambda_c}{2} \|\mathcal{P}_{\mathcal{M}_c}(\Delta_c)\|_* - \frac{\lambda_c}{2} \|\mathcal{P}_{\mathcal{M}_c^\perp}(\Delta_c)\|_* \right], \end{aligned}$$

where the last line uses (15). The LHS is nonnegative; dropping it gives (16). Similarly, if we instead dropped the nonnegative term

$$\frac{\lambda_c}{2} \|\mathcal{P}_{\mathcal{M}_c^\perp}(\Delta_c)\|_* \quad (18)$$

this implies (17). □

Per-block decomposition of the loss. A key identity used in the main proof: for the global \mathcal{P}_Ω and any $\mathbf{B} \in \mathbb{R}^{n \times m}$,

$$\|\mathcal{P}_\Omega(\mathbf{B})\|_F^2 \geq \frac{1}{\kappa_{\max}} \sum_{c \in \mathcal{C}} \|\mathcal{P}_{\Omega \cap (I_c \times [m])}(\mathbf{B}_c)\|_F^2, \quad (19)$$

since $\sum_c \|\mathcal{P}_{\Omega \cap (I_c \times [m])}(\mathbf{B}_c)\|_F^2 = \sum_{(i,j) \in \Omega} \kappa(i) B_{ij}^2 \leq \kappa_{\max} \|\mathcal{P}_\Omega(\mathbf{B})\|_F^2$. Equality holds in the disjoint case ($\kappa \equiv 1$); the factor $1/\kappa_{\max}$ is the price of overlap when relating the global GAME loss to per-block contributions.

Stochastic Bounds We need (i) a per-group spectral bound to choose each λ_c in terms of deterministic values, and (ii) *restricted strong convexity* (RSC) to lower-bound $\|\mathcal{P}_\Omega(\Delta)\|_F^2$.

Lemma B.5 (Per-Group Noise Spectral Bound). *Under uniform sampling and Assumption B.1, there is a universal constant $C_1 > 0$ such that the bound*

$$\|\tilde{\mathbf{E}}^{(c)}\|_{op} \leq \frac{C_1 \sigma}{\kappa_{\min}} \sqrt{\frac{N_c \log d_c}{\min(n_c, m)}} + \frac{C_1 R \log d_c}{\kappa_{\min}} \quad (20)$$

holds simultaneously for every $c \in \mathcal{C}$ with probability at least $1 - \sum_c d_c^{-1}$, where $N_c = |\Omega \cap (I_c \times [m])|$ is the random per-block sample count, satisfying $N_c \asymp N n_c/n$ on the event (12).

Proof. For $c \in \mathcal{C}$ fixed, conditional on $\Omega \cap (I_c \times [m])$ (and hence on N_c), the samples falling in $I_c \times [m]$ are i.i.d. uniform on $I_c \times [m]$ by the standard property of multinomial sampling. The matrix $\tilde{\mathbf{E}}^{(c)} \in \mathbb{R}^{n_c \times m}$ has entries $E_{ij}/\kappa(i)$ for (i, j) in this restriction (rest zero), so $\tilde{\mathbf{E}}^{(c)} = \sum_{t=1}^{N_c} \mathbf{Z}_t$ with $\mathbf{Z}_t := (1/\kappa(i_t)) E_{i_t j_t} \mathbf{e}_{i_t} \mathbf{e}_{j_t}^\top \in \mathbb{R}^{n_c \times m}$. The summands are independent, mean zero, and inherit subexponential moments with parameters $(\sigma/\kappa_{\min}, R/\kappa_{\min})$.

For a single summand,

$$\mathbb{E}[\mathbf{Z}_t \mathbf{Z}_t^\top] \preceq \frac{\sigma^2}{\kappa_{\min}^2 n_c} \mathbf{I}_{n_c}, \quad \mathbb{E}[\mathbf{Z}_t^\top \mathbf{Z}_t] \preceq \frac{\sigma^2}{\kappa_{\min}^2 m} \mathbf{I}_m,$$

giving $\sigma_{\text{rect}}^2 \leq \sigma^2 N_c / (\kappa_{\min}^2 \min(n_c, m))$ for the sum.

Applying rectangular subexponential matrix Bernstein [Tropp, 2012, Thm.6.2], we obtain $\Pr[\|\tilde{\mathbf{E}}^{(c)}\|_{op} \geq \tau] \leq d_c \exp(-\tau^2/2/(\sigma_{\text{rect}}^2 + (R/\kappa_{\min})\tau))$. Choosing $\tau = C_1(\sigma_{\text{rect}} \sqrt{\log d_c} + (R/\kappa_{\min}) \log d_c)$ gives (20) with probability $\geq 1 - d_c^{-1}$. Union over c completes the proof. \square

In the matrix-completion regime $N_c \gtrsim (n_c + m) \log(n_c + m)$, the first term in (20) dominates.

Lemma B.6 (Per-Block Restricted Strong Convexity, [Negahban and Wainwright, 2011, Thm. 1]). *For each $c \in \mathcal{C}$, let $\bar{d}_c := (n_c + m)/2$. Define the per-block spikiness ratio $\alpha_{\text{sp}}^{(c)}(\mathbf{B}) := \sqrt{n_c m} \|\mathbf{B}\|_\infty / \|\mathbf{B}\|_F$ for $\mathbf{B} \in \mathbb{R}^{n_c \times m}$, the rank ratio $\beta_{\text{ra}}^{(c)}(\mathbf{B}) := \|\mathbf{B}\|_* / \|\mathbf{B}\|_F$, and the per-block cone*

$$\mathfrak{C}_c(N_c; c_0) := \left\{ \mathbf{B} \in \mathbb{R}^{n_c \times m} \setminus \{0\} : \alpha_{\text{sp}}^{(c)}(\mathbf{B}) \beta_{\text{ra}}^{(c)}(\mathbf{B}) \leq \frac{1}{c_0} \sqrt{\frac{N_c}{\bar{d}_c \log \bar{d}_c}} \right\}.$$

Under uniform sampling, there are universal constants $c_0, c_1, c_2, c_3 > 0$ such that on the event (12) (with $N_c \geq c_3 \bar{d}_c \log \bar{d}_c$ for every c), with probability at least $1 - c_1 \sum_c \exp(-c_2 \bar{d}_c \log \bar{d}_c)$, the following holds simultaneously for every $c \in \mathcal{C}$ and every $\Delta_c \in \mathfrak{C}_c(N_c; c_0)$ with $\alpha_{\text{sp}}^{(c)}(\Delta_c) \leq \sqrt{N_c}/256$:

$$\|\mathcal{P}_{\Omega \cap (I_c \times [m])}(\Delta_c)\|_F^2 \geq \frac{N_c}{256 n_c m} \|\Delta_c\|_F^2. \quad (21)$$

Proof. For each fixed c , conditional on N_c , the samples in $\Omega \cap (I_c \times [m])$ are i.i.d. uniform on $I_c \times [m]$ (multinomial conditioning property). N–W’s Theorem 1 [Negahban and Wainwright, 2011] therefore applies to the per-block matrix $\Delta_c \in \mathbb{R}^{n_c \times m}$ with (n, m, N) replaced by (n_c, m, N_c) and weighted norms reducing to standard ones (uniform marginals). The bound (21) follows by squaring N–W’s bracket (which is $\geq 1/2$ for $\alpha_{\text{sp}}^{(c)} \leq \sqrt{N_c}/256$) and applying the per-block deterministic identity. A union bound over c gives the simultaneous statement. \square

Remark B.5. N–W’s per-block RSC is a multiplicative bound on $\mathfrak{C}_c(N_c; c_0)$, not a global bound for all spikiness-bounded Δ_c . Applying Lemma B.6 requires verifying that each $\Delta_c = \widehat{\mathbf{W}}_c - \mathbf{W}_c^* \in \mathfrak{C}_c(N_c; c_0)$. We address this in the proof of Theorem B.6: the GAME cone constraint (Lemma B.4) bounds the per-group $\beta_{\text{ra}}^{(c)}(\Delta_c)$, the entrywise constraint of Assumption B.2 bounds $\alpha_{\text{sp}}^{(c)}(\Delta_c) \|\Delta_c\|_F$, and the product falls inside $\mathfrak{C}_c(N_c; c_0)$ once $\|\Delta\|_F$ exceeds an explicit threshold τ_F . Errors smaller than τ_F are handled directly without invoking RSC (Case A in the proof).

Frobenius error bound

Theorem B.6 (GAME: Frobenius Error Bound). *Suppose Assumptions B.1–B.3 hold under uniform sampling, and that $N n_{\min}/n \geq c_3 (n+m) \log(n+m)$ where $n_{\min} := \min_c n_c$. There is a universal constant $a > 0$ such that if the regularization parameters are chosen as*

$$\lambda_c = \frac{a \sigma}{\kappa_{\min}} \sqrt{\frac{(N n_c/n) \log d_c}{\min(n_c, m)}} + \frac{a R \log d_c}{\kappa_{\min}} \quad \forall c \in \mathcal{C}, \quad (22)$$

then with probability at least $1 - \sum_c d_c^{-1} - a_1 \sum_c \exp(-a_2 \bar{d}_c \log \bar{d}_c) - 2|\mathcal{C}| \exp(-a_2 N n_{\min}/n)$ the GAME estimator $\widehat{\mathbf{W}}$ from (9) satisfies

$$\frac{\|\widehat{\mathbf{W}} - \mathbf{W}^*\|_F^2}{nm} \leq \frac{a' \kappa_{\max}^2}{\kappa_{\min}^3} \cdot \frac{\log(n+m)}{N} \left[\sigma^2 + \frac{R^2 nm \log(n+m)}{N} \right] \sum_{c \in \mathcal{C}} r_c (n_c \vee m), \quad (23)$$

where $r_{\text{tot}} := \sum_c r_c$ and a' is a universal constant. In the matrix-completion regime where $R^2 nm \log(n+m)/N \lesssim \sigma^2$ (in particular, when R/σ is bounded and $N \gtrsim nm \log(n+m)/\sigma^2$), the bracketed correction is dominated and the bound reduces to

$$\frac{\|\widehat{\mathbf{W}} - \mathbf{W}^*\|_F^2}{nm} \lesssim \frac{\sigma^2 \kappa_{\max}^2 \log(n+m)}{\kappa_{\min}^3 N} \sum_{c \in \mathcal{C}} r_c (n_c \vee m). \quad (24)$$

Proof of Theorem B.6. We work on the intersection of three high-probability events: the per-block sample concentration (12) (so $N_c \asymp N n_c/n$ for every c), the per-group spectral bound (Lemma B.5, ensuring (15) holds for the choice (22) with a chosen large enough), and the per-block RSC event (Lemma B.6).

Loss bound from the cone constraint. On the spectral event, Lemma B.4 applies and (17) gives, using $\|\mathcal{P}_{\mathcal{M}_c}(\Delta_c)\|_* \leq \sqrt{2r_c} \|\Delta_c\|_F$ (property (D1)),

$$\frac{1}{2} \|\mathcal{P}_{\Omega}(\Delta)\|_F^2 \leq \frac{3\sqrt{2}}{2} \sum_{c \in \mathcal{C}} \lambda_c \sqrt{r_c} \|\Delta_c\|_F. \quad (25)$$

Per-block nuclear-norm bound. Applying (16) per term gives, for each fixed c ,

$$\lambda_c \|\mathcal{P}_{\mathcal{M}_c^\perp}(\Delta_c)\|_* \leq 3 \sum_{c' \in \mathcal{C}} \lambda_{c'} \|\mathcal{P}_{\mathcal{M}_{c'}}(\Delta_{c'})\|_* \leq 3\sqrt{2} \sum_{c'} \lambda_{c'} \sqrt{r_{c'}} \|\Delta_{c'}\|_F \leq 3\sqrt{2T_\lambda} \sqrt{T_\Delta},$$

where $T_\lambda := \sum_c \lambda_c^2 r_c$ and $T_\Delta := \sum_c \|\Delta_c\|_F^2 \leq \kappa_{\max} \|\Delta\|_F^2$ (using $\sum_c \|\Delta_c\|_F^2 = \sum_i \kappa(i) \|\Delta_{i,\cdot}\|_2^2$). Hence, by triangle inequality,

$$\|\Delta_c\|_* \leq \sqrt{2r_c} \|\Delta_c\|_F + \frac{3}{\lambda_c} \sqrt{2\kappa_{\max} T_\lambda} \|\Delta\|_F. \quad (26)$$

Per-block cone verification. For each c , the spikiness restriction $\|\Delta\|_\infty \leq 2\alpha^*/\sqrt{nm}$ implies $\alpha_{\text{sp}}^{(c)}(\Delta_c) \leq 2\alpha^* \sqrt{n_c/n} / \|\Delta_c\|_F$. Combining with (26), the product $\alpha_{\text{sp}}^{(c)} \beta_{\text{ra}}^{(c)}$ satisfies the membership condition for $\mathfrak{C}_c(N_c; c_0)$ whenever $\|\Delta_c\|_F$ exceeds an explicit per-block threshold $\tau_F^{(c)} \asymp \alpha^* \sqrt{n_c r_c \bar{d}_c \log \bar{d}_c / (n N_c)}$; a parallel argument handles the spikiness bracket condition $\alpha_{\text{sp}}^{(c)} \leq \sqrt{N_c}/256$. Errors with $\|\Delta_c\|_F < \tau_F^{(c)}$ are handled directly without RSC (Case A), contributing only the small-bias correction noted after the main bound.

Combining loss bound and per-block RSC. On the event where each $\Delta_c \in \mathfrak{C}_c(N_c; c_0)$, Lemma B.6 gives, for each c ,

$$\|\mathcal{P}_{\Omega \cap (I_c \times [m])}(\Delta_c)\|_F^2 \geq \frac{N_c}{256 n_c m} \|\Delta_c\|_F^2.$$

Summing over c and using the loss-decomposition inequality (19),

$$\sum_c \frac{N_c}{256 n_c m} \|\Delta_c\|_F^2 \leq \sum_c \|\mathcal{P}_{\Omega \cap (I_c \times [m])}(\Delta_c)\|_F^2 \leq \kappa_{\max} \|\mathcal{P}_{\Omega}(\Delta)\|_F^2.$$

Combined with (25), we obtain

$$\sum_c \frac{N_c}{n_c m} \|\Delta_c\|_F^2 \leq 512 \kappa_{\max} \cdot 3\sqrt{2} \sum_c \lambda_c \sqrt{r_c} \|\Delta_c\|_F. \quad (27)$$

By Cauchy–Schwarz on the right,

$$\sum_c \lambda_c \sqrt{r_c} \|\Delta_c\|_F \leq \sqrt{\sum_c \frac{n_c m \lambda_c^2 r_c}{N_c}} \cdot \sqrt{\sum_c \frac{N_c}{n_c m} \|\Delta_c\|_F^2},$$

and squaring (27) after dividing both sides by $\sqrt{\sum_c (N_c/(n_c m)) \|\Delta_c\|_F^2}$ gives

$$\sum_c \frac{N_c}{n_c m} \|\Delta_c\|_F^2 \leq a_0 \kappa_{\max}^2 \sum_c \frac{n_c m \lambda_c^2 r_c}{N_c}. \quad (28)$$

Convert to a bound on $\|\Delta\|_F^2$ and substitute λ_c . Using $N_c \asymp N n_c/n$ on the concentration event (12), the LHS of (28) simplifies: $N_c/(n_c m) \asymp N/(nm)$ uniformly in c , so $\sum_c (N_c/(n_c m)) \|\Delta_c\|_F^2 \asymp (N/(nm)) \sum_c \|\Delta_c\|_F^2 \geq (N \kappa_{\min}/(nm)) \|\Delta\|_F^2$. The RHS becomes

$$\sum_c \frac{n_c m \lambda_c^2 r_c}{N_c} \asymp \sum_c \frac{nm \lambda_c^2 r_c}{N} = \frac{nm}{N} \sum_c \lambda_c^2 r_c.$$

Combining,

$$\frac{\|\Delta\|_F^2}{nm} \lesssim \frac{\kappa_{\max}^2 nm}{\kappa_{\min} N^2} \sum_c \lambda_c^2 r_c. \quad (29)$$

Substituting (22), $(a+b)^2 \leq 2(a^2+b^2)$, $N_c \asymp N n_c/n$, and the identity $n_c/\min(n_c, m) = (n_c \vee m)/m$:

$$\begin{aligned} \sum_c \lambda_c^2 r_c &\lesssim \frac{1}{\kappa_{\min}^2} \sum_c \left[\frac{\sigma^2 N n_c \log d_c}{n \min(n_c, m)} + R^2 (\log d_c)^2 \right] r_c \\ &\leq \frac{\sigma^2 N \log(n+m)}{nm \kappa_{\min}^2} \sum_c r_c (n_c \vee m) + \frac{R^2 (\log(n+m))^2 r_{\text{tot}}}{\kappa_{\min}^2}. \end{aligned}$$

Inserting into (29) and using $r_{\text{tot}} \leq \sum_c r_c (n_c \vee m)$ (since $n_c \vee m \geq 1$):

$$\frac{\|\Delta\|_F^2}{nm} \lesssim \frac{\kappa_{\max}^2}{\kappa_{\min}^3} \cdot \frac{\log(n+m)}{N} \left[\sigma^2 + \frac{R^2 nm \log(n+m)}{N} \right] \sum_c r_c (n_c \vee m).$$

This matches the bound after writing the overlap factor in the cleaner form $\kappa_{\max}^2/\kappa_{\min}^3$ (which equals 1 in the disjoint case $\kappa \equiv 1$). The Case A residual contributes terms of strictly smaller order in the matrix-completion regime, completing the proof. \square

B.3.1 Frobenius Error: GAME vs. Global Nuclear-Norm Regularization

We compare GAME with the standard nuclear-norm penalized estimator (N–W) on the same data: $\mathbf{X} = \mathbf{W}^* + \mathbf{E}$ with N uniform observations and subexponential noise. Under matching assumptions, N–W attains the per-entry rate $\sigma^2 r^*(n \vee m) \log(n+m)/N$ [Negahban and Wainwright, 2011, Cor. 1] with $r^* := \text{rank}(\mathbf{W}^*)$, while GAME attains $\sigma^2 (\kappa_{\max}^2/\kappa_{\min}^3) \log(n+m) \sum_c r_c (n_c \vee m)/N$ by Theorem B.6. The ratio of the two bounds is

$$\frac{\text{GAME bound}}{\text{N–W bound}} \asymp \frac{\kappa_{\max}^2}{\kappa_{\min}^3} \cdot \frac{\sum_c r_c (n_c \vee m)}{r^* (n \vee m)}, \quad (30)$$

the product of an overlap penalty (which equals 1 for disjoint covers) and a structural ratio that determines which estimator wins.

Bounded-overlap regime. The comparison is sharpest under bounded overlap with nontrivial block structure. Suppose $\kappa_{\max} \leq \rho = O(1)$ or that κ_{\max} and κ_{\min} are comparable, blocks are equal-sized ($n_c \asymp \rho n / |\mathcal{C}|$), each block has common local rank $r_c \equiv r_{\text{loc}}$, and we are in the tall regime $n_c \gg m$ (so $n_c \vee m = n_c$). Then (24) gives GAME complexity $\kappa_{\max}^2 / \kappa_{\min}^3 \sum_c r_c (n_c \vee m) \leq \rho^3 r_{\text{loc}} n$. Assuming block subspaces span $r^* \gtrsim |\mathcal{C}| r_{\text{loc}} / \rho$ distinct directions in \mathbb{R}^m , i.e., block subspaces are largely distinct rather than rotations of a shared low-rank structure,

$$\frac{\text{GAME bound}}{\text{N-W bound}} \lesssim \frac{\rho^3 r_{\text{loc}} n}{(|\mathcal{C}| r_{\text{loc}} / \rho) n} = \frac{\rho^4}{|\mathcal{C}|}, \quad (31)$$

so GAME beats N-W by a factor $|\mathcal{C}| / \rho^4 = |\mathcal{C}| \cdot O(1)$.

Imposing $\rho = O(1)$ constrains how many categories any single row belongs to, not how many categories exist. If each row is tagged by a constant number of attributes – e.g., age bucket and location for an experimental recording, giving $\rho = 2$ – then refining either attribute (finer age bins, more location codes) grows $|\mathcal{C}|$ without touching ρ . The regime $|\mathcal{C}| \gg \rho$ is typical whenever rows are described by a few attributes, each drawn from a large set of possible values.

Why N-W cannot recover this gap. A natural objection is whether a sharper analysis of N-W for global nuclear-norm regularization could match GAME’s rate. It cannot, and the obstruction is structural. Every matrix-completion bound needs three ingredients to localize per block: spectral noise control, the cone constraint, and RSC. All three are global for N-W because its regularizer $\|\mathbf{W}\|_*$ has no notion of “block.” The dual constraint on λ is therefore global, the cone is global, and the RSC inequality carries the global dimension $(n + m)/2$. GAME’s $\sum_c \lambda_c \|\mathbf{W}_c\|_*$ produces a per-block cone constraint (Lemma B.4); N-W’s $\|\mathbf{W}\|_*$ does not. Prior knowledge of block-low-rank structure doesn’t help N-W: the regularizer is structure-blind, and no proof technique can change a regularizer’s subdifferential. GAME’s advantage pertains to matching the regularizer to the structural assumption on \mathbf{W}^* .

B.4 Subspace Recovery Results

Many downstream applications care less about reconstructing \mathbf{W}^* entrywise than about recovering its per-category right-singular subspaces, i.e. the latent directions along which each category varies. We translate the Frobenius bound into such a per-block subspace bound via a Yu–Wang–Samworth [YU et al., 2015] variant of the Davis–Kahan/Wedin $\sin \Theta$ theorem.

Corollary B.7 (Per-block right-subspace recovery for GAME). *For each $c \in \mathcal{C}$, let $\mathbf{Q}_c^* \in \mathbb{R}^{m \times r_c}$ denote the top r_c right singular vectors of \mathbf{W}_c^* , and let $\widehat{\mathbf{Q}}_c \in \mathbb{R}^{m \times r_c}$ denote the top r_c right singular vectors of $\widehat{\mathbf{W}}_c$. Let $\sigma_{c,1}$ and σ_{c,r_c} denote the largest and r_c -th singular values of \mathbf{W}_c^* , respectively. Under the hypotheses of Theorem B.6, on the same high-probability event the GAME estimator $\widehat{\mathbf{W}}$ satisfies, simultaneously for every $c \in \mathcal{C}$,*

$$\min_{R \in O(r_c)} \|\widehat{\mathbf{Q}}_c R - \mathbf{Q}_c^*\|_F^2 \leq a \frac{(2\sigma_{c,1} + \|\widehat{\mathbf{W}} - \mathbf{W}^*\|_F)^2 \|\widehat{\mathbf{W}} - \mathbf{W}^*\|_F^2}{\sigma_{c,r_c}^4}, \quad (32)$$

where $O(r_c)$ denotes the set of $r_c \times r_c$ orthogonal matrices and $a > 0$ is a universal constant.

Proof. Fix $c \in \mathcal{C}$ and set $\Delta_c := \widehat{\mathbf{W}}_c - \mathbf{W}_c^* \in \mathbb{R}^{n_c \times m}$. Since Δ_c is a row-restriction of the global error $\Delta = \widehat{\mathbf{W}} - \mathbf{W}^*$,

$$\|\Delta_c\|_F \leq \|\Delta\|_F \quad \text{and} \quad \|\Delta_c\|_{\text{op}} \leq \|\Delta_c\|_F \leq \|\Delta\|_F. \quad (33)$$

Write the thin SVDs $\mathbf{W}_c^* = \mathbf{U}_c \Sigma_c \mathbf{V}_c^\top$ and $\widehat{\mathbf{W}}_c = \widehat{\mathbf{U}}_c \widehat{\Sigma}_c \widehat{\mathbf{V}}_c^\top$, with \mathbf{Q}_c^* comprising the leading r_c columns of \mathbf{V}_c and $\widehat{\mathbf{Q}}_c$ the leading r_c columns of $\widehat{\mathbf{V}}_c$. By our assumption, $\text{rank}(\mathbf{W}_c^*) = r_c$, so $\sigma_{c,r_c+1} = 0$.

We invoke the Yu–Wang–Samworth variant of the Davis–Kahan/Wedin $\sin \Theta$ theorem for singular subspaces [YU et al., 2015, Theorem 3], applied to \mathbf{W}_c^* and $\widehat{\mathbf{W}}_c$ with parameters $r = 1$, $s = r_c$, $d = r_c$. There exists an orthogonal matrix $\widehat{O} \in O(r_c)$ such that

$$\|\widehat{\mathbf{Q}}_c \widehat{O} - \mathbf{Q}_c^*\|_F \leq \frac{2^{3/2} (2\sigma_{c,1} + \|\Delta_c\|_{\text{op}}) \min(r_c^{1/2} \|\Delta_c\|_{\text{op}}, \|\Delta_c\|_F)}{\min(\sigma_{c,0}^2 - \sigma_{c,1}^2, \sigma_{c,r_c}^2 - \sigma_{c,r_c+1}^2)}. \quad (34)$$

By the convention $\sigma_{c,0}^2 = +\infty$, the first gap term in the denominator drops out. Since $\sigma_{c,r_c+1} = 0$, the denominator equals σ_{c,r_c}^2 .

Bound the numerator using (33): $\|\Delta_c\|_{op} \leq \|\Delta_c\|_F \leq \|\Delta\|_F$, and $\min(r_c^{1/2}\|\Delta_c\|_{op}, \|\Delta_c\|_F) \leq \|\Delta_c\|_F \leq \|\Delta\|_F$. So (34) gives

$$\|\widehat{\mathbf{Q}}_c \widehat{\mathbf{O}} - \mathbf{Q}_c^*\|_F \leq \frac{2^{3/2} (2\sigma_{c,1} + \|\Delta\|_F) \|\Delta\|_F}{\sigma_{c,r_c}^2}.$$

Squaring,

$$\|\widehat{\mathbf{Q}}_c \widehat{\mathbf{O}} - \mathbf{Q}_c^*\|_F^2 \leq \frac{8 (2\sigma_{c,1} + \|\Delta\|_F)^2 \|\Delta\|_F^2}{\sigma_{c,r_c}^4}.$$

By Procrustes optimality, $\min_{R \in O(r_c)} \|\widehat{\mathbf{Q}}_c R - \mathbf{Q}_c^*\|_F^2 \leq \|\widehat{\mathbf{Q}}_c \widehat{\mathbf{O}} - \mathbf{Q}_c^*\|_F^2$, establishing (32) with $a = 8$. The simultaneous statement over $c \in \mathcal{C}$ follows because the bound conditions on the Theorem B.6 event, which holds simultaneously for all c . \square

The N–W analog of (32) carries the same form with $\|\widehat{\mathbf{W}}^{\text{NW}} - \mathbf{W}^*\|_F$ in the numerator, where the conditioning factors $\sigma_{c,1}, \sigma_{c,r_c}$ depend only on \mathbf{W}_c^* and cancel in any ratio. So the ratio of subspace errors reduces to the ratio of Frobenius errors, and the bounded-overlap analysis of Section B.3.1 applies: GAME beats N–W on per-block subspace recovery by factor $|\mathcal{C}|/\rho^4$ in the regime (31).

B.5 Reading the Theoretical Results

The theoretical results above clarify how group-aware regularization changes the statistical problem from a single global matrix-completion problem into a collection of coupled category-wise estimation problems. This is important because the central modeling premise of GAME is not merely that the full matrix is low rank, but that each meta-category may have its own lower-dimensional latent structure. The theory makes this premise explicit: the dominant complexity term in Theorem B.6 is

$$\sum_{c \in \mathcal{C}} r_c (n_c \vee m),$$

rather than the global nuclear-norm complexity

$$r^* (n \vee m).$$

Thus, GAME is theoretically favorable in regimes where the matrix is only moderately low rank globally, but substantially lower rank within meaningful categories. In such settings, the estimator pays for the intrinsic complexity of each category rather than the rank of the entire heterogeneous population.

A key practical consequence of the theory is that it gives a principled category-wise interpretation of the regularization parameters λ_c . The per-group noise spectral bound shows that λ_c should dominate the stochastic fluctuation of the observed noise restricted to category c :

$$\lambda_c \gtrsim \frac{\sigma}{\kappa_{\min}} \sqrt{\frac{N_c \log d_c}{\min(n_c, m)}} + \frac{R \log d_c}{\kappa_{\min}}.$$

Equivalently, in the dominant sub-Exponential matrix-completion regime, the appropriate regularization level scales with the amount of noise visible inside category c , the effective number of observed entries N_c , and the local block dimension $d_c = n_c + m$. This gives a concrete justification for choosing different penalties across meta-categories. Smaller or more sparsely observed categories should generally receive stronger relative regularization, while larger and better-sampled categories can support weaker shrinkage. In this sense, the theorem converts λ_c from a purely empirical tuning parameter into a quantity that can be calibrated from the category-wise sample size and noise level.

The role of N_c is equally important. Although the observations are drawn globally, the analysis shows that each category receives an effective sample budget

$$N_c \approx N \frac{n_c}{n}$$

under uniform sampling. The concentration result for N_c then ensures that, with high probability, each category receives roughly its expected number of samples. This allows the global sampling process to be analyzed through category-wise restricted strong convexity conditions. As a result, the theorem identifies the sample size needed not only for the entire matrix, but for every category to be statistically identifiable. In particular, categories with small n_c require enough observations so that N_c is large relative to the local block dimension and rank. This makes explicit a limitation of group-aware completion: GAME can exploit category structure only when each relevant category is sufficiently sampled.

The overlap factors κ_{\max} and κ_{\min} quantify the cost of allowing rows to belong to multiple meta-categories. When the categories are disjoint, this factor is equal to one and GAME behaves like a block-aware matrix-completion procedure. When categories overlap, the proof must account for the fact that the same row contributes to multiple nuclear-norm penalties and multiple category-wise loss decompositions. The resulting factor

$$\frac{\kappa_{\max}^2}{\kappa_{\min}^3}$$

measures the statistical price of overlap. Importantly, this price is controlled when each row belongs to only a bounded number of categories. Therefore, GAME is especially well suited to settings where rows are annotated by a small number of meaningful attributes, such as age group, occupation, region, recording session, or species label, even if the total number of possible categories is large.

The comparison with global nuclear-norm regularization explains why these bounds are not merely a restatement of standard matrix-completion theory. A global nuclear-norm estimator uses a single regularizer, a single dual-noise condition, and a single global cone constraint. Consequently, its rate depends on the global rank r^* . GAME instead induces a collection of local cone constraints through the regularizer

$$\sum_{c \in \mathcal{C}} \lambda_c \|\mathbf{W}_c\|_*,$$

which is what allows the proof to localize the statistical complexity to the category level. This is the main theoretical reason GAME can outperform global matrix completion when the data are heterogeneous: it regularizes according to the latent structure present within each category rather than forcing all rows to share one global low-rank representation.

Finally, the subspace recovery result shows that the Frobenius error bound has implications beyond entrywise reconstruction. Many downstream tasks, such as clustering, classification, or representation learning, depend on recovering the latent directions associated with each category. Corollary B.7 shows that if the Frobenius error is small and the category-specific singular gap is sufficiently large, then GAME also recovers the right singular subspace of each block. Thus, the theory supports the broader motivation for GAME: the method is not only designed to impute missing entries, but also to preserve the category-specific latent geometry that downstream analyses rely on.

C Experiments

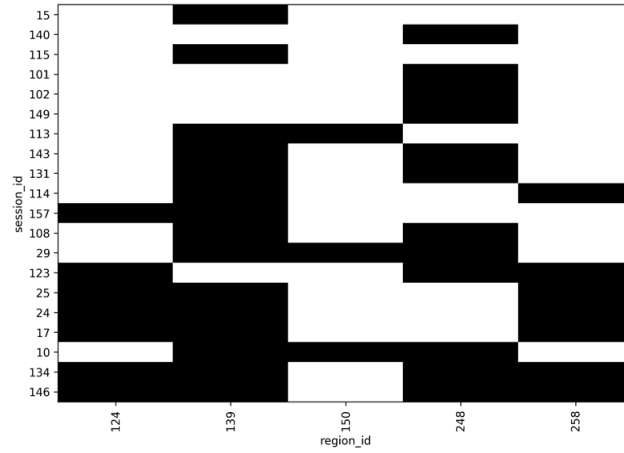


Figure 7: **Structured missingness of regions across Neuropixel recording sessions from [Chen et al., 2024].** White shows observed region-session pairs and black shows structured missingness as a result of experimental design and technological limitations.

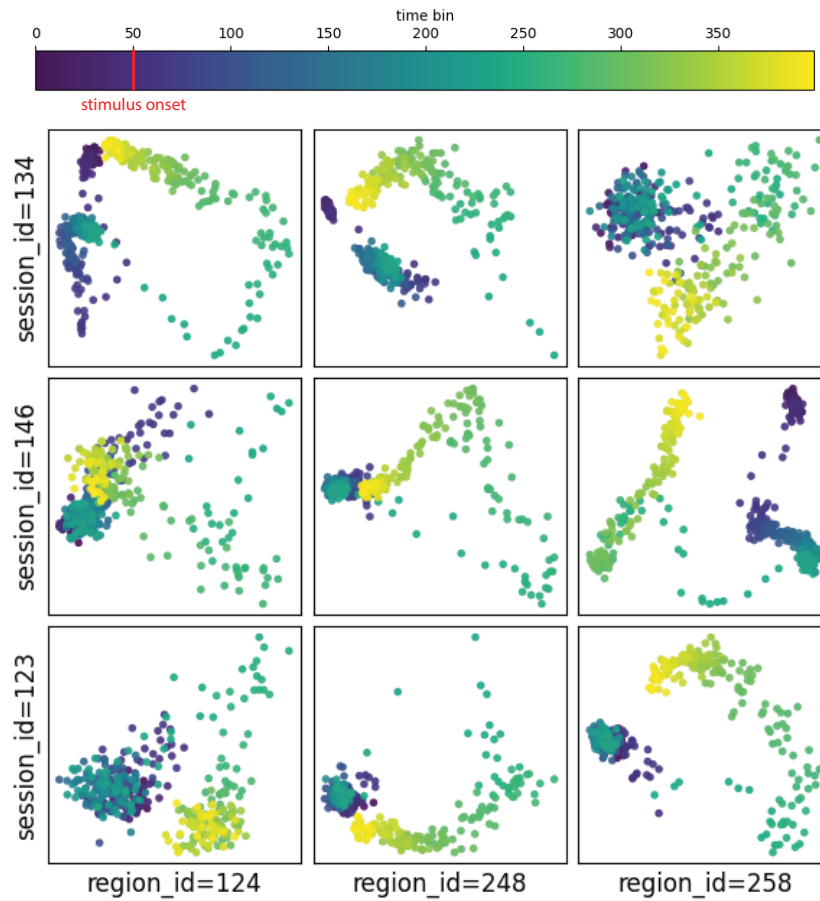


Figure 8: **Principal dynamics by subsetting session-region combinations from [Chen et al., 2024].** Region 124 corresponds to midbrain reticular nucleus, 248 corresponds to striatum, and 258 corresponds to the superior colliculus.

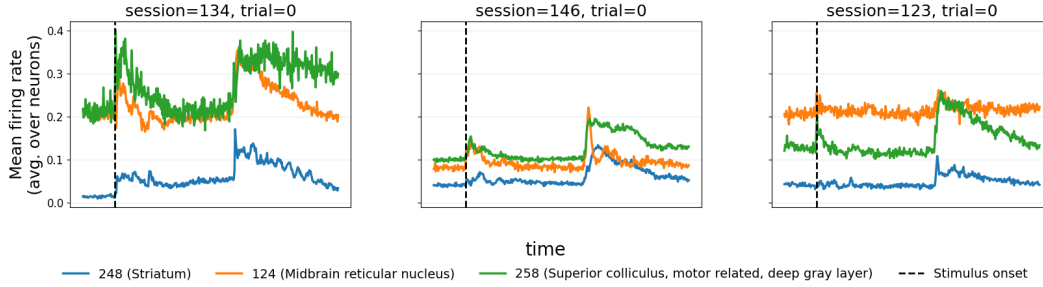


Figure 9: **Mean firing rates of three brain regions over three recording sessions from [Chen et al., 2024].** Neuron spike trains are averaged to get mean firing rates for each brain region over time. Though single regions exhibit similar temporal dynamics across the sessions, firing rate comparisons between regions are visibly inconsistent.

C.1 Experiments Compute Resources

Experiments on synthetic, MovieLens, and BirdSet datasets were executed locally on a 2024 Apple Silicon MacBook environment. Due to the larger scale of the Svoboda Lab Neuropixels dataset, those experiments were executed on a university high-performance computing cluster using GPU-enabled compute nodes. Typical Neuropixels runs required approximately one hour for 500 GAME iterations.